AD_____

Award Number: W81XWH-04-1-0456

TITLE: Manipulation of NF-KappaB Activity in the Macrophage Lineage as a Novel Therapeutic Approach

PRINCIPAL INVESTIGATOR: Fiona E. Yull, Ph.D.

CONTRACTING ORGANIZATION: Vanderbilt University Medical Center
Nashville, TN 37203-6917

REPORT DATE: May 2007

TYPE OF REPORT: Annual

PREPARED FOR: U.S. Army Medical Research and Materiel Command
Fort Detrick, Maryland 21702-5012

REPORT DOCUMENTATION PAGE

Form Approved
OMB No. 0704-0188

1. REPORT DATE *(DD-MM-YYYY)*	**2. REPORT TYPE**	**3. DATES COVERED** *(From - To)*
01-05-2007	Annual	19 Apr 2006 – 18 Apr 2007

4. TITLE AND SUBTITLE

Manipulation of NF-KappaB Activity in the Macrophage Lineage as a Novel Therapeutic Approach

5a. CONTRACT NUMBER

5b. GRANT NUMBER
W81XWH-04-1-0456

5c. PROGRAM ELEMENT NUMBER

6. AUTHOR(S)

Fiona E. Yull, Ph.D.

E-Mail: Fiona.Yull@vanderbilt.edu

5d. PROJECT NUMBER

5e. TASK NUMBER

5f. WORK UNIT NUMBER

7. PERFORMING ORGANIZATION NAME(S) AND ADDRESS(ES)

Vanderbilt University Medical Center
Nashville, TN 37203-6917

8. PERFORMING ORGANIZATION REPORT NUMBER

9. SPONSORING / MONITORING AGENCY NAME(S) AND ADDRESS(ES)
U.S. Army Medical Research and Materiel Command
Fort Detrick, Maryland 21702-5012

10. SPONSOR/MONITOR'S ACRONYM(S)

11. SPONSOR/MONITOR'S REPORT NUMBER(S)

12. DISTRIBUTION / AVAILABILITY STATEMENT
Approved for Public Release; Distribution Unlimited

13. SUPPLEMENTARY NOTES - original document contains color figures.

14. ABSTRACT

Morphogenesis of the mammary gland is a highly complex process which when misregulated can result in tumorigenesis. It involves the interactions of multiple cell types in a highly regulated manner with complex signal transduction pathways coordinating the physiological processes. Interactions between epithelial and mesenchymal cells are known to be important. Recent studies highlight the importance of cell types, such as macrophages. The nuclear factor-kappa B (NF-kB) family of transcription factors appears to be critical in regulating the dynamic changes during normal and neoplastic development. This proposal seeks to investigate the contribution of NF-kB signaling within macrophages in normal and neoplastic mammary development. Our data will provide insights into the importance of NF-kB signaling in macrophages for tumor development and progression and have the potential for identification of novel therapeutic strategies. During this period we continued to characterize macrophages with constitutive NF-kappaB activity and identified differences in proliferation rates, expression of downstream gene expression and effects mediated by altered macrophages on associated epithelial cells. In addition, we have obtained the 3rd novel transgenic necessary for an inducible system to make feasible manipulation of NF-kappaB activity in macrophages in vivo. We have generated the double transgenics necessary to test our new models and have preliminary data to suggest that altered NF-kappaB activity within macrophages has significant effects on mammary ductal development.

15. SUBJECT TERMS
NF-kappaB, macrophages, mammary ductal development, doxycycline inducible transgenics

16. SECURITY CLASSIFICATION OF:			**17. LIMITATION OF ABSTRACT**	**18. NUMBER OF PAGES**	**19a. NAME OF RESPONSIBLE PERSON**
a. REPORT	**b. ABSTRACT**	**c. THIS PAGE**			USAMRMC
U	U	U	UU	22	**19b. TELEPHONE NUMBER** *(include area code)*

Standard Form 298 (Rev. 8-98)
Prescribed by ANSI Std. Z39.18

Table of Contents

INTRODUCTION

Morphogenesis of the mammary gland is a highly complex process which when misregulated can result in tumorigenesis. It involves the interactions of multiple cell types in a highly regulated manner with complex signal transduction pathways coordinating the physiological processes. Interactions between epithelial and mesenchymal cells are known to be important. However, recent studies are beginning to highlight the importance of other cell types, such as macrophages. One of the signaling molecules that appears to be critical in regulating the dynamic changes during normal and neoplastic development is the nuclear factor-kappa B (NF-□) family of transcription factors. NF-□B can regulate many genes that are expressed by macrophages that are important for proliferation and apoptosis of cells, as well as remodeling and angiogenesis. This proposal seeks to investigate the contribution of NF-□B signaling within macrophages in defining the macrophage's role in normal and neoplastic mammary development. The proposed experiments use multiple murine lines and novel assay systems. These studies will provide information regarding the signaling pathways involved in normal mammary development. They will also provide insights into the importance of NF-□B signaling in macrophages for tumor development and progression and will have the potential for identification of novel therapeutic strategies.

BODY

Task 1. To investigate the effects of constitutive NF-□B activity within macrophages on mammary development (Months 1-24):

a. Perform fetal liver cell transplantation using I□B-□ null and control donors at postnatal day 19 to determine effects on virgin postnatal mammary development of constitutive NF-□B activity in reconstituted hematopoietic cells (Months 1-24). [100 mice]
b. Perform fetal liver cell transplantation using I□B-□ null and control donors into recipients at 6 weeks. Allow hematopoetic cell reconstitution for a further 6 weeks. Mate recipient mice and investigate effects on development during pregnancy of constitutive NF-□B activity in hematopoietic cells (Months 1-24). [100 mice]

In last years report we described a number of technical concerns with the fetal liver transplantation technique and our intention to focus ongoing efforts on development of the inducible model proposed as aim 2.

While our intention was to focus the majority of our efforts on development of the inducible model (Aim 2) we have continued to use our I□B-□ null model to continue *in vitro* strategies. In last years report we discussed generation of immortalized bone marrow derived cell lines from our novel NGL reporter mice. We also reported western analysis of nuclear and cytoplasmic extracts from primary bone marrow cells from I□B-□ +/- and wildtype mice demonstrating an increased LPS responsiveness in extracts from +/- mice. In order to carry out more extensive and targeted cell culture studies based on the I□B-□ null model, we have since generated immortalized bone marrow derived macrophage cell lines from both wild type and I□B-alpha null mice. While I□B-□ wild type macrophages appear typically small and spherical, the morphological appearance of the I□B-□ -/- cells is different. These cells are larger and often multinucleated (Figure 1A). Treatment of the cells with M-CSF exacerbates the observed morphological phenotype. MTT assay to determine proliferation rate of wild type and I□B-□ -/- macrophages determined that knockout cells proliferate at approximately twice the rate of wild type cells ($p<0.001$) (Figure 1B).

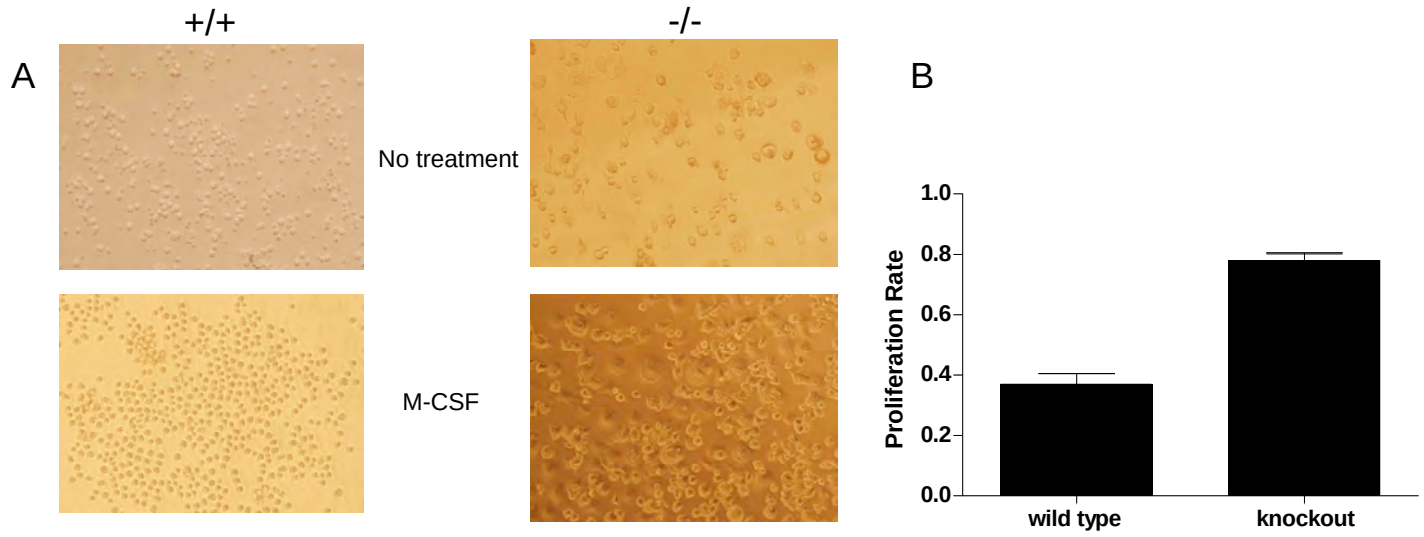

Figure 1A – cultured wild type and I□B-□ -/- macrophage cell lines display different morphological phenotypes and responses to stimuli (M-CSF), B – MTT assay highlights differences in proliferation rates between wild type and knockout cell lines.

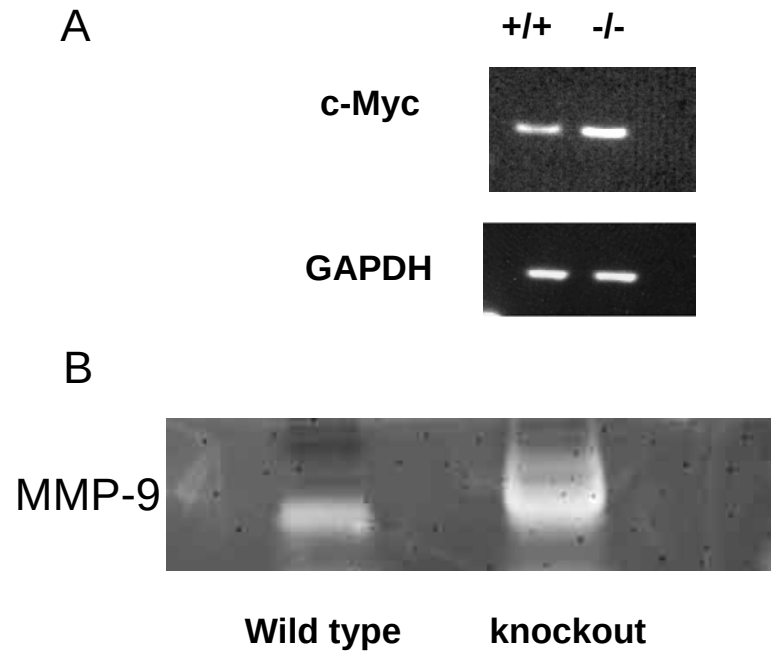

Figure 2A - RT-PCR shows increased levels of c-Myc expression in knockout cell lines. **B**- Gel zymography of conditioned medium (48hrs) from wild type and I□B-□ knockout macrophages.

We were interested in determining potential downstream NF-□B target genes whose differential expression could be contributing to the observed differences in proliferation rates. RT-PCR analysis suggests that c-myc mRNA expression is increased in I□B-□ -/- compared to wild type cells, implicating c-Myc as one of the important target genes whose expression is altered by the constitutive NF-□B activity (Figure 2A). Another target gene that can be regulated by NF-□B signaling is matrix metalloproteinase-9 (MMP-9). The regulation of MMP activity is known to be important in epithelial cell branching and normal mammary gland development (Witty et al., 1995; Simian et al., 2001). The expression and activity of MMPs is also associated with mammary tumors and human breast cancer where they contribute to invasion and metastasis (Egeblad and Werb, 2002; Heppner et al., 1996). In addition, the expression of MMP-9 has been demonstrated to require activation of NF-□B (Bond et al., 1998) and we have recently shown that MMP-9 activity is affected during postnatal mammary development by NF-□B signaling (Connelly et al., 2007). Given these correlations between NF-□B signaling and mammary development and tumorigenesis we decided to investigate the production of MMP-9 by the macrophage cell lines. Gel zymography and densitometric analysis show a 2-fold increase in MMP-9 in media conditioned by I□B-□ -/- macrophages compared to wild type cells (Figure 2B).

Finally for this section we were interested in the potential for macrophages in which NF-κB signaling was altered to impact the behavior of adjacent mammary epithelial cells. In order to begin to investigate this, we cultured normal mammary epithelial cells (NMuMG) in conditioned medium from our macrophage cell lines. Interestingly, our preliminary data suggest that the cells cultured in medium from knockout macrophages may survive more effectively than those cultured in wild type medium (Figure 3). This provides some evidence that altered macrophages can impact associated epithelium but requires further investigation.

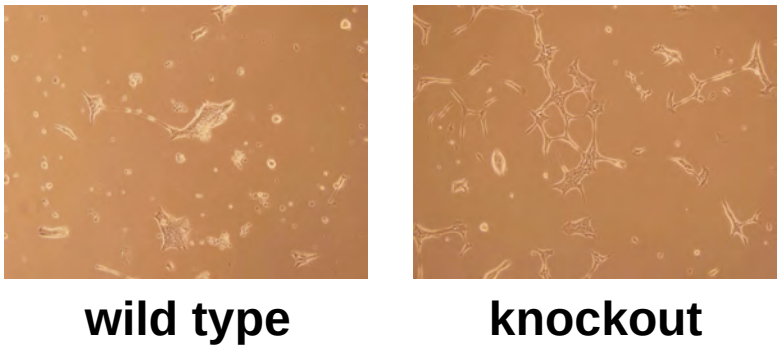

Figure 3. NMuMG mammary epithelial cells cultured for 48 hrs in conditioned medium from wild type or IκBζ knockout macrophages.

The goal of these studies is to investigate the contribution of NF-κB signaling within macrophages in defining the macrophage's role in normal and neoplastic mammary development. Summarizing the data from this section, we have established cell lines from wild type and knockout IκB-ζ mice. Using these cell lines we have obtained data concerning the effects of constitutive NF-κB signaling on macrophage cells themselves including increased proliferation rates and increased levels of expression of genes that are known to play roles in both normal development and tumorigenesis. In addition, we have obtained preliminary data to suggest that the macrophages with the altered behavior are able to produce mediators that alter the behavior of mammary epithelial cells. Clearly a great deal more investigation is required to determine the specific mediators and whether these effects are on survival, proliferation or motility of the epithelial cells.

Task 2. Assess effects on mammary development of induced and inhibited NF-κB activity using novel inducible transgenics (Months 1-36).

a. Investigate postnatal development in doxycycline-induced macrophage-restricted constitutive activator double transgenic mice (IKMRP) and controls (Months 1-36). [300 mice]
b. Investigate postnatal development doxycycline-induced macrophage-restricted dominant inhibitor double transgenic mice in (DNMRP) and controls (Months 1-36). [300 mice]

In collaboration with the group of Dr Timothy Blackwell, we have been developing conditional transgenic modular mouse models, based on the tetracycline inducible system, to over-express IκB-DN (dominant inhibitor) or cIKK2 (constitutive activator) in response to treatment with doxycycline in drinking water. The components of this system include transgenics expressing the reverse tetracycline transactivator (rtTA) in the appropriate cell type, and transgenics in which the tetracycline operator $(tet\text{-}O)_7$ and a minimal CMV promoter drive expression of either the dominant inhibitor (IκB-DN), or a constitutively active IKK2 mutant. Key DNA components for the system were obtained from Dr Jay Tichelaar (Perl et al., 2002). In the presence of doxycycline, the rtTA binds to tet-O and induces downstream gene expression within 24 hours. In these transgenics, the IκB-DN construct that we have has mutations of the critical phosphorylation targets (serine residues) that are normally phosphorylated in response to signaling resulting in degradation of the inhibitor (Chen et al., 1999). This mutated form of inhibitor is not degraded in response to phosphorylation signals and therefore functions to block NF-κB signaling. To facilitate detection of induced transgene products we have attached a FLAG tag to the cIKK2 and a Myc-His tag to the dominant inhibitor. The transgenics expressing the inhibitor are named DN. The transgenics expressing the activator are named IKK. In order to modulate expression in macrophages, we collaborated with the group of Dr. John Christman (formerly at Vanderbilt and

now in Chicago). We designed a transgenic construct to achieve macrophage restricted expression of the reverse tetracycline transactivator (rtTA)(Perl et al., 2002). Expression was targeted to macrophages using a promoter based on the mannose receptor promoter (MRP)(Eichbaum et al., 1997) and including 3 repeats of a PU.1 responsive element (DeKoter et al., 2000). The transactivator transgenics were named MRP. With the assistance of the Vanderbilt Transgenic/ES Cell Shared Resource we generated 4 independent lines each of the DN, IKK and MRP transgenics.

We have now completed extensive collaborative studies using the DN and IKK transgenics crossed with an existing, well-characterized lung-specific CC-10rtTA transgenic (Perl et al., 2002). We previously reported testing all 4 lines of IKK transgenics and all 4 lines of DN transgenics in crosses with the lung specific rtTA and extensive characterization of these lines. The DN and IKK transgenes are functional and able to modulate NF-κB activity *in vivo*. We have used the lung-targeted form of the modular inducible transgenic system in collaborative studies that have been accepted for publication in the Journal of Immunology (see appended manuscript).

We also generated 4 independent lines of MRP transgenics. We generated double transgenic animals carrying a combination of the DN and MRP transgenes (DNMP) or the IKK and MRP transgenes (IKMP) and previously reported our efforts to detect induced expression targeted to the macrophage lineage. While we were able to detect expression by RT-PCR we were unable to detect expression at the protein level by western analysis despite our ability to easily detect induced expression in the lung targeted system using the same antibodies. We also completed a very minimal set of studies in which we treated DNMP and IKMP double transgenics with 2g/l doxycycline in drinking water from 4-8 weeks of age, harvested mammary glands and completed whole mount analyses. Our intention was to determine whether perhaps there were low levels of expression that may be sufficient to produce a phenotype even in the absence of detectable protein expression by western. However, no differences were detected between double transgenics and controls. Taking into consideration all of our data we were forced to conclude that the four lines of MRP transgenics do not result in sufficient expression of the rtTA to be of use for the inducible system.

As our proposed research would benefit greatly from having the inducible system within macrophages we sought an alternative strategy. The c-fms gene encodes the receptor for macrophage colony-stimulating factor (CSF-1). The c-fms promoter has been successfully used to generate macrophage specific transgenics (Sasmono et al., 2003; Burnett et al., 2004). In trying to find a source for this promoter we made contact with Professor Michael Ostrowski at Ohio State University, Columbus, Ohio. We discovered that his research group are also attempting to make a macrophage-targeted rtTA transgenic. They had founder animals from two different transgene constructs each of which uses a different form of the c-fms promoter. Both types of transgenics express high levels of the transgene as determined by RT-PCR. Dr. Ostrowski kindly agreed to collaborate with us and at the time of last year's report representative males from the two different types of founder lines were being serology tested for transfer to our facility.

We have since obtained the founder animals and mated them with our IKK and DN transgenics to determine whether they have sufficient levels of rtTA expression to be effective in our inducible system. Initially we decided to determine whether we could detect expression of the IKK transgene in *ex vivo* cell culture experiments. We took two double positive IKFM (cfms and IKK) and two control mice and extracted BMDMs, cultured in medium containing M-CSF for 10 days (method according to Connelly et al. 2003). The cells were seeded in 6-well plates and stimulated with doxycycline (1µg/ml) for 24 and 48 hours. Whole cell protein extracts were prepared and western blot analyses performed to detect FLAG-IKK. Despite attempts to load a relatively large amount of protein we were unable to detect a band of the correct size that would indicate successful induction of IKK expression.

In order to extend the period of treatment and optimize the probability of transgene induction, we took one double positive IKFM and one DNFM mouse and controls and administered doxycycline (2g/L) in drinking water for 1 week. Bone marrow cells were harvested and seeded in 6-well plates in the presence of M-CSF and 100ng/ml doxycycline. 100ng/ml doxycycline was added every 2 days to culture medium. Cells were collected at 6, 8 and 10 days from each line and whole cell protein extracts prepared. Western blot analyses were performed using appropriate antibodies to detect FLAG-IKK and myc-DN. Once again, we were unable to detect induced protein expression.

We contacted Dr. Ostrowski for reassurance that the c-fms-rtTA transgenic was functional. They have been performing studies using the inducible system to express Cre recombinase and have detected recombined products in macrophage cells (data not shown).

We were concerned about our inability to specifically detect transgene at the level of protein expression and decided to adopt an RT-PCR strategy to attempt to detect transgene expression at the level of RNA.

We have treated two DNFM double positives and two control animals with 2g/L doxycycline in drinking water for 4 weeks. Lung, liver and intestine tissue samples have been harvested from each animal and snap frozen in liquid nitrogen. Bronchioalveolar and peritoneal lavage have been completed and bone marrow cells harvested from femurs (pooled cells from double positives and controls to provide one sample from each). All the above tissue samples will be used to prepare RNA and perform RT-PCR. We have designed and are in the process of optimizing the use of new primer pairs to detect FLAG-IKK and DN-Myc by RT-PCR. We have carried out a preliminary study using the new primers designed to detect induced expression of the DN transgene (Figure 4). While this strategy requires some additional optimization and the inclusion of controls such as DNFM double positive mice in the absence of dox treatment, we believe that the preliminary data is promising. We also harvested mammary glands to perform whole mount analyses.

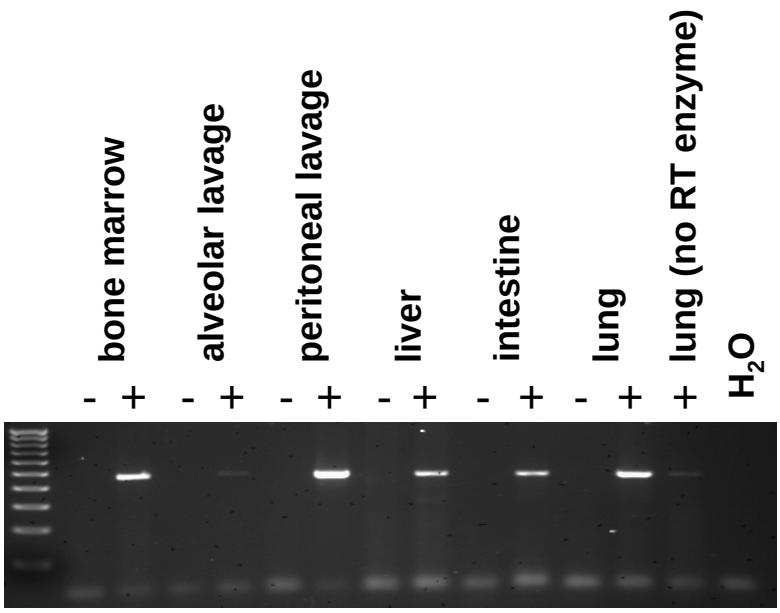

Figure 4 - RT-PCR for DN transgene in DNFM (double positives) and controls (double negative). DNFM mice were treated with 2g/L doxycycline in drinking water for 4 weeks before tissue collecion

In a similar approach we have also treated two IKFM double positives and two controls with 2g/L doxycycline in drinking water for 4 weeks. We have harvested lung, liver and intestine tissue samples from each animal, snap frozen tissues in liquid nitrogen, and harvested bone marrow from femurs. Mammary glands were harvested for whole mount analyses. We have also designed and are in the process of optimizing the use of new primer pairs to detect FLAG-IKK by RT-PCR.

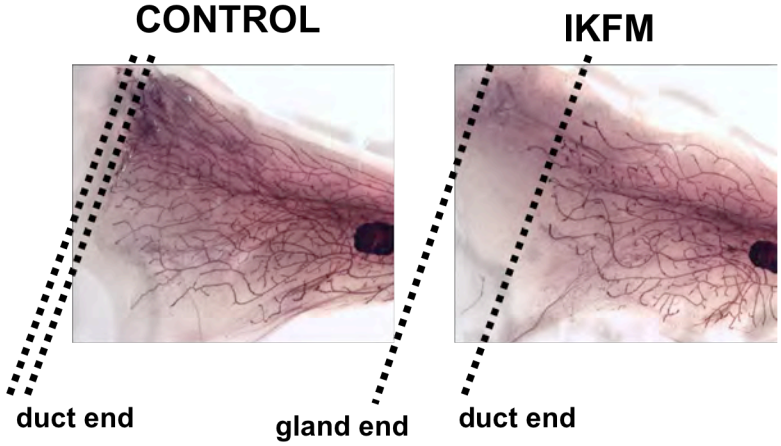

Figure 5 - Whole mount analyses of control and double IKFM transgenics following treatment with doxycycline from week 4-8.

We decided that it was possible that the transgene was being induced but at low levels that were below the detection limits of our western analysis. Therefore, we treated one IKFM double positive and 2 control mice with 2g/L doxycycline in drinking water from 4 to 8 weeks of age. The mammary glands were harvested and whole mount analysis performed. In these very preliminary studies we have observed a different phenotype in double positive as compared to controls (Figure 5). At this early stage we would describe the phenotype as an inhibited invasion of the virgin ductal growth into the mammary fat pad.

We have performed a similar strategy to assess whether phenotypic effects can be observed by treatment of doxycycline to induce the DN transgene in macrophages. In this preliminary study we treated one DNFM double positive and one control mouse with 2g/L doxycycline in drinking water from 4 to 8 weeks of age (Figure 6). The mammary glands were harvested and whole mount analyses performed. In this preliminary study we also observed a different phenotype in the double positive as compared to the control glands. In this instance from this preliminary study we would describe the phenotype as the persistence of relatively large terminal ductal end structures.

At this point, we are optimistic that the inducible model is functional and will produce worthwhile data.

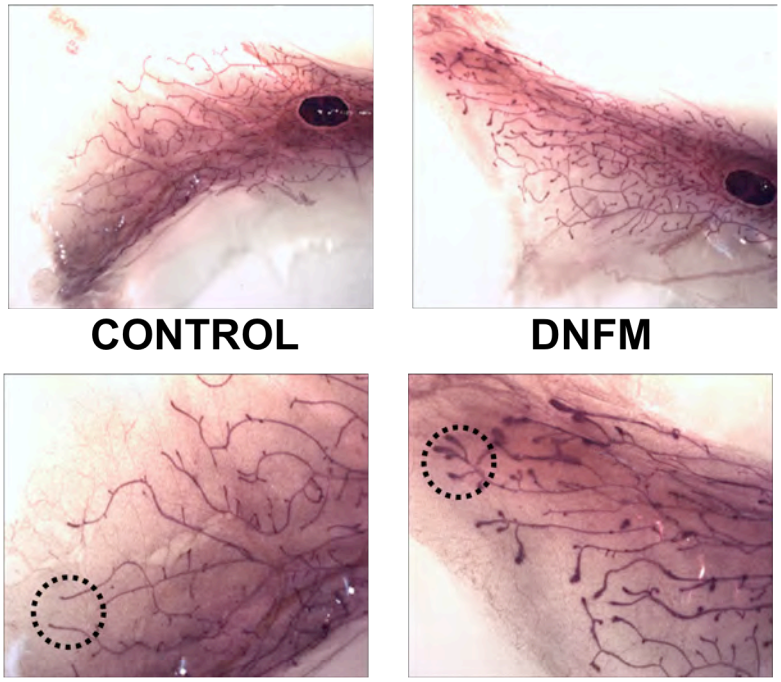

Figure 6 - Whole mount analyses of control and double DNFM transgenics following treatment with doxycycline from week 4-8.

Task 3. To determine whether manipulation of NF-□B activity within macrophage populations effects tumorigenesis (Months 25-36).

a. Investigate effects on tumorigenesis in PyMT/IKMRP doxycycline-induced transgenics and controls. ie. does constitutive NF-□B activity within macrophages exacerbate tumorigenesis? (Months 25-36). [100 mice]
b. Investigate effects on tumorigenesis in PyMT/DNMRP doxycycline-induced transgenics and controls. ie. does reduced NF-□B activity within macrophages inhibit tumorigenesis? (Months 25-36). [100 mice]

As originally proposed this task was dependent on establishing the model described in task 2 and was not scheduled to commence until month 25. However, due to the difficulties we have experienced in establishing the critical macrophage targeted rtTA transgenic component of the inducible modular system we adopted an intermediate strategy to obtain worthwhile data in the event that we were unsuccessful in developing the modular system in time to make significant progress with this aim.

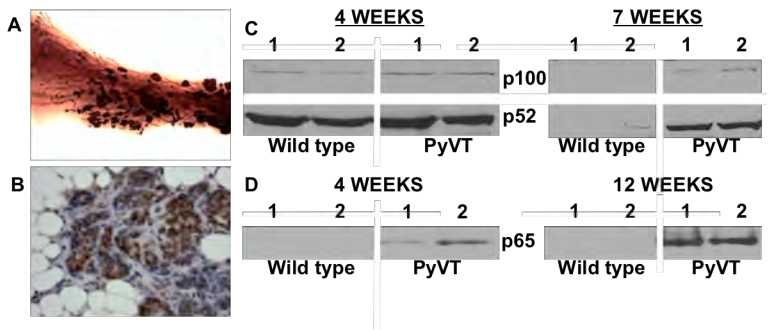

Figure 7. A. Mammary gland whole mount from 7 week old PyVT transgenic. **B**. Immunohistochemistry for GFP in mammary section from 7 week old PyVT/NGL transgenic. **C.** Western blot for p100 and p52 in mammary gland whole cell extract from wild type and PyVT. **D.** Western blot for p65 in mammary gland nuclear extracts from wild type and PyVT.

We obtained the PyMT transgenic mice and established a small colony. While this model of mammary cancer has been used in a number of studies, little is known concerning the pattern of NF-□B activation during the development of the tumors. Our new NGL reporter transgenics provide us with a unique opportunity to investigate the stages during tumor progression in which NF-□B is active and the specific cell types involved. We have commenced breeding the PyMT transgenics with the NGL reporter

transgenics to enable us to investigate the pattern of NF-□B activation at the various stages of tumor development (Figure 7). The PyVT mice rapidly develop mammary tumors that are readily visible in whole mount analyses by 7 weeks of age (Figure 7A). Using immunohistochemistry to detect GFP expression in double PyVT/NGL reporter transgenics we are able to visualize localized NF-□B activation within the developing mammary tumors (Figure 7B). Our reporter transgenics do not distinguish between activation of the classical and alternative NF-□B pathways. Therefore, we completed western blot analyses to detect p52/p100 expression (alternative pathway) and translocation of p65 to the nucleus (classical pathway) (Figure 7C + D). These data provide an intriguing hint about the roles of the two pathways in mammary tumor development. Activation of the alternative signaling pathway occurs via processing of the p100 protein to the shorter p52 form. This pathway is active in both control and PyVT mammary tissue at 4 weeks. At this stage, we believe that this represents activation of a pathway that is important for normal ductal development. However, signaling via the alternative pathway appears to shut down in control animals but be maintained in PyVT mice at 7 weeks. This may indicate that part of the mechanism by which the PyVT induces tumor formation is by maintaining a normal developmental signal, extended into an inappropriate period. Elevated activation of the classical pathway has been associated with breast tumors and cell lines. Thus the activation of this pathway in tissue samples that bear developing mammary tumors was somewhat expected. Interestingly, activation of this pathway was not detected in control tissues.

In order to be in a position to rapidly commence some of the original proposed studies should the new macrophage transgenics prove effective, we have generated homozygous forms of the IKK and DN transgenics to facilitate optimized breeding strategies.

KEY RESEARCH ACCOMPLISHMENTS

During this reporting period;

1) We have generated immortalized macrophage cell lines from I□B-□ -/- and wild type mice. We have characterized the behavior of the cell lines that have constitutive NF-□B activity and identified effects on cellular proliferation, expression of downstream target genes and the ability of these cells to influence behavior of adjacent epithelial cells.
2) In collaboration with the group of Dr. Timothy Blackwell, we have generated transgenics in which either the dominant inhibitor or a constitutive activator of NF-□B is under the control of an inducible promoter and confirmed that they are functional. These transgenics have now been fully characterized, have been used in collaborative studies and have been included in an accepted manuscript (see reportable outcomes).
3) We have obtained potential macrophage targeted rtTA transgenic mice from the laboratory of Professor M. Ostrowski, Ohio State University and our preliminary characterization of these transgenics when crossed with our inducible activator and inhibitor transgenics suggests that they may result in interesting and informative phenotypes.
4) We have established a colony of PyVT transgenics and established double PyVT/NGL transgenics. Using these mice we have been able to begin to characterize the patterns of NF-□B signaling during mammary tumor development in this model.

REPORTABLE OUTCOMES

Our collaborative efforts with the laboratory of Dr. Timothy Blackwell have led to a publication during the reporting period.

Airway epithelium controls development of acute lung injury through the NF-□B pathway (2007). Cheng, D-S.C., Han, W., Chen, S., Sherrill, T.P., Chont, M., Park, G-Y., Sheller, J.R., Polosukhin, V.V., Christman, J.W., Yull, F.E., and Blackwell, T.S. J Immunology 178:6504-13 (the last two authors contributed equally).

CONCLUSIONS

In summary, we have generating and characterized 3 of the 4 originally proposed transgenics. Collaborative studies with the reporter NGL, constitutive activator IKK and dominant inhibitor DN transgenics have led to one additional accepted publication. We have amended our strategy to utilize our novel IκB-ε -/- model using them to generate macrophage cell lines. These cell lines are enabling us to gain insights into the specific effects of altered NF-κB activity on macrophages themselves and their influence on adjacent epithelial cells. This data is relevant to both normal mammary development and tumorigenesis. While we encountered difficulties in the generation of the 4th transgenic (the macrophage targeted rtTA) we are collaborating with Dr M Ostrowski and have started the characterization of these new transgenics in combination with our DN and IKK inducible transgenics. The available data suggests that these inducible models are functional and may result in significant phenotypes. We have also obtained data suggesting that both the classical and alternative pathways may be active during tumor development in the Polyoma model but with differential patterns of activity potentially indicative of specific roles.

Our original time frame would have ended the grant period at this time. However, generation of the critical macrophage-targeted rtTA transgenic was delayed but now appears within reach. Therefore, we have requested and been approved for a no-cost extension period to enable us to complete characterization of this model with remaining funds. We continue to be optimistic that our approaches will reveal an important role for NF-κB signaling within macrophages on both normal development and tumorigenesis and lead to further publications within the extended time frame of this funding.

REFERENCES

Beg, A.A., Sha, W.C., Bronson, R.T., Baltimore, D. (1995) Constitutive NF-kappa B activation, enhanced granulopoiesis, and neonatal lethality in I kappa B alpha-deficient mice. *Genes Dev*. 9:2736-46.

Bond, M., Fabunmi, R. P., Baker, A. H., and Newby, A. C. (1998) Synergistic upregulation of metalloproteinase-9 by growth factors and inflammatory cytokines: an absolute requirement for transcription factor NF-kappa B. *FEBS Lett* **435**(1), 29-34.

Burnett, S.H., Kershen, E.J., Zhang, J., Zeng, L., Straley, S.C., Kaplan, A.M., Cohen, D.A. (2004) Conditional macrophage ablation in transgenic mice expressing a Fas-based suicide gene. *J Leukoc Biol.* 75:612-23.

Chen, C-L., Yull, F.E., Kerr, L.D. (1999) Differential serine phosphorylation regulates IkB-a inactivation. *Biochem. Biophys. Res. Comm*. 257, 798-806.

Chen, C-L., Singh, N., Yull, F.E., Strayhorrn, D., Van Kaer, L., Kerr, L.D. (2000). Lymphocytes lacking IκB-ε develop normally, but have selective defects in proliferation and function. *Journal of Immunology* 165: 5418-5427.

Chen, C-L., Yull, F.E., Cardwell, N., Nanney, L., Kerr, L.D. (2000b) RAG2-/-, IκB-ε-/- chimeras display a psoriasis-like skin disease. *Journal of Investigative Dermatology*, 115: 1124-1133.

Connelly, L., Jacobs, A.T., Palacios-Callender, M., Moncada, S. & Hobbs A.J. (2003). Macrophage endothelial nitric oxide synthase auto-regulates cellular activation and pro-inflammatory protein expression. *J. Biol. Chem.*, 278: 26480-26487.

Connelly, L., Robinson-Benion, C., Chont, M., Saint-Jean, L., Li, H., Polosukhin, V.V., Blackwell, T.S., Yull, F.E. (2007) A transgenic model reveals important roles for the NF-kappaB alternative pathway (p100/p52) in mammary development and links to tumorigenesis. *J Biol Chem.* 282: 10028-35.

DeKoter, R.P., Singh, H. (2000). Regulation of B lymphocyte and macrophage development by graded expression of PU.1. *Science.* 288: 1439-41.

Eichbaum, Q., Heney, D., Raveh, D., Chung, M., Davidson, M., Epstin, J., Ezekowitz, A.B. (1997) Murine macrophage mannose receptor promoter is regulated by the transcription factors PU.1 and SP1. Blood 90: 4135-143.

Egeblad, M., and Werb, Z. (2002) New functions for the matrix metalloproteinases in cancer progression. *Nat Rev Cancer* **2**(3), 161-174.
Everhart, M.B., Han, W., Parman, K.S., Polosukhin, VV., Zeng, H., Sadikot, R.T., Li, B., Yull, F.E., Christman, J.W., Blackwell, T.S. 2005. Intratracheal administration of liposomal clodronate accelerates alveolar macrophage reconstitution following fetal liver transplantation. *J Leukoc Biol.* 77:173-80.
Everhart, M.B., Han, W., Sherrill, T.P., Arutiunov, M., Polosukhin, V.V., Burke, J.R., Sadikot, R.T., Christman, J.W., Yull, F.E., Blackwell, T.S. Duration and Intensity of NF-{kappa}B Activity Determine the Severity of Endotoxin-Induced Acute Lung Injury. J Immunol. 2006 176:4995-5005.
Heppner, K. J., Matrisian, L. M., Jensen, R. A., and Rodgers, W. H. (1996) Expression of most matrix metalloproteinase family members in breast cancer represents a tumor-induced host response. *Am J Pathol* **149**(1), 273-282.
Klement, J.F., Rice, N.R., Car, B.D., Abbondanzo, S.J., Powers, G.D., Bhatt, P.H., Chen, C.H., Rosen, C.A., Stewart, C.L. (1996) IkappaBalpha deficiency results in a sustained NF-kappaB response and severe widespread dermatitis in mice. *Mol Cell Biol*. 16:2341-9.
Sasmono, R.T., Oceandy, D., Pollard, J.W., Tong, W., Pavli, P., Wainwright, B.J., Ostrowski, M.C., Himes, S.R., Hume, D.A. (2003) A macrophage colony-stimulating factor receptor-green fluorescent protein transgene is expressed throughout the mononuclear phagocyte system of the mouse. *Blood* 101:1155-63.
Perl, A.K., Tichelaar, J.W., Whitsett, J.A. (2002) Conditional gene expression in the respiratory epithelium of the mouse. *Transgenic Research*. 11:21-9.
Sadikot, R.T., Zeng, H., Joo, M., Everhart, M.B., Sherrill, T.P., Li, B., Cheng, D.S., Yull, F.E., Christman, J.W., Blackwell, T.S. (2006) Targeted Immunomodulation of the NF-{kappa}B Pathway in Airway Epithelium Impacts Host Defense against Pseudomonas aeruginosa. *J Immunol*. 176:4923-30.
Simian, M., Hirai, Y., Navre, M., Werb, Z., Lochter, A., and Bissell, M. J. (2001) The interplay of matrix metalloproteinases, morphogens and growth factors is necessary for branching of mammary epithelial cells. *Development* **128**(16), 3117-3131.
Witty, J. P., Wright, J. H., and Matrisian, L. M. (1995) Matrix metalloproteinases are expressed during ductal and alveolar mammary morphogenesis, and misregulation of stromelysin-1 in transgenic mice induces unscheduled alveolar development. *Mol Biol Cell* **6**(10), 1287-1303.

APPENDICES

Airway epithelium controls development of acute lung injury through the NF-□B pathway (2007). Cheng, D-S.C., Han, W., Chen, S., Sherrill, T.P., Chont, M., Park, G-Y., Sheller, J.R., Polosukhin, V.V., Christman, J.W., Yull, F.E., and Blackwell, T.S. J Immunology 178:6504-13 (note that last two authors contributed equally to the publication).

Airway Epithelium Controls Lung Inflammation and Injury through the NF-κB Pathway[1]

Dong-sheng Cheng,* Wei Han,* Sabrina M. Chen,* Taylor P. Sherrill,* Melissa Chont,† Gye-Young Park,¶ James R. Sheller,* Vasiliy V. Polosukhin,* John W. Christman,§¶ Fiona E. Yull,[2†] and Timothy S. Blackwell[2,3]*†‡§

Although airway epithelial cells provide important barrier and host defense functions, a crucial role for these cells in development of acute lung inflammation and injury has not been elucidated. We investigated whether NF-κB pathway signaling in airway epithelium could decisively impact inflammatory phenotypes in the lungs by using a tetracycline-inducible system to achieve selective NF-κB activation or inhibition in vivo. In transgenic mice that express a constitutively active form of IκB kinase 2 under control of the epithelial-specific CC10 promoter, treatment with doxycycline induced NF-κB activation with consequent production of a variety of proinflammatory cytokines, high-protein pulmonary edema, and neutrophilic lung inflammation. Continued treatment with doxycycline caused progressive lung injury and hypoxemia with a high mortality rate. In contrast, inducible expression of a dominant inhibitor of NF-κB in airway epithelium prevented lung inflammation and injury resulting from expression of constitutively active form of IκB kinase 2 or *Escherichia coli* LPS delivered directly to the airways or systemically via an osmotic pump implanted in the peritoneal cavity. Our findings indicate that the NF-κB pathway in airway epithelial cells is critical for generation of lung inflammation and injury in response to local and systemic stimuli; therefore, targeting inflammatory pathways in airway epithelium could prove to be an effective therapeutic strategy for inflammatory lung diseases. ***The Journal of Immunology,*** **2007, 178: 6504–6513.**

The NF-κB pathway impacts a number of key biological processes, including innate immunity, through transcriptional regulation of target genes. Following cell stimulation, IκBs are phosphorylated on serine residues in the amino terminus by IκB kinase 2 (IKK2),[4] targeting them for destruction by the ubiquitin/proteasome (26S) degradation pathway (1). IκB degradation allows NF-κB nuclear translocation and transcriptional activation of a variety of genes, including cytokines, chemokines, and adhesion molecules (2, 3). In the lungs, many noxious/inflammatory stimuli have been shown to activate NF-κB, including bacterial products, ozone and silica, as well as systemic inflammatory insults such as sepsis, trauma, and hemorrhage.

Innate immunity is critical for host defense against bacterial pathogens, but dysregulated or exaggerated immune responses can result in tissue injury. In the lungs, this form of host-derived tissue injury characterizes the acute respiratory distress syndrome (ARDS). ARDS is a common cause of morbidity and mortality in critically ill patients, resulting from local or systemic infection, trauma, or other inflammatory/injurious stimuli (4, 5). The inflammatory phenotype underlying the pathogenesis of ARDS includes neutrophilic alveolitis and increased levels of a number of cytokines and chemokines in the airways (4, 6). Improved understanding of critical cell types and biological pathways that regulate innate immunity in the lungs could be useful in designing therapies to limit or prevent lung injury in patients at risk for ARDS.

Airway epithelium provides a physical border between host and environment that protects from injurious and infectious stimuli that gain access to the respiratory tract through inspiration or aspiration. Well-recognized functions of airway epithelium include mechanical clearance of offending agents and production of antimicrobial agents; however, critical functions for coordinating the innate immune response or development of lung injury have not been identified. Airway epithelial cells express a number of TLRs, and we have recently shown that local and systemic inflammation results in prominent activation of the NF-κB pathway in these cells (7–9). Therefore, we hypothesized that epithelial cells in the lung are important for transducing NF-κB-dependent inflammatory signals and that prolonged NF-κB activation in airway epithelial cells leads to a dysfunctional (injurious) inflammatory response culminating in lung injury. To evaluate whether airway epithelial cells critically regulate lung inflammation and injury, we generated inducible transgenic mice that express an activator or dominant inhibitor of the NF-κB pathway in CC10-expressing airway epithelial cells. We then determined the effects of cell type-specific NF-κB activation or inhibition on parameters of lung inflammation and injury. Our data indicate that activation of NF-κB in airway

*Division of Allergy, Pulmonary and Critical Care Medicine, Department of Medicine, †Department of Cancer Biology, and ‡Department of Cell and Developmental Biology, Vanderbilt University School of Medicine, Nashville, TN 37232; and §Department of Veterans Affairs and ¶Section of Pulmonary, Critical Care, and Sleep Medicine, University of Illinois, Chicago, IL 60605

Received for publication November 9, 2006. Accepted for publication March 1, 2007.

The costs of publication of this article were defrayed in part by the payment of page charges. This article must therefore be hereby marked *advertisement* in accordance with 18 U.S.C. Section 1734 solely to indicate this fact.

[1] This work was supported by National Institutes of Health Grants HL61419, HL66196, and HL07123; the U.S. Department of Veterans Affairs; Vanderbilt Ingram Cancer Center; Susan G. Komen Foundation Grant BCTR02-1728; and Department of Defense Breast Cancer Program Grant WX1XWH-04-1-0456.

[2] F.E.Y. and T.S.B. contributed equally to this manuscript.

[3] Address correspondence and reprint requests to Dr. Timothy S. Blackwell, Vanderbilt University School of Medicine, T-1218 MCN, Nashville, TN 37232. E-mail address: timothy.blackwell@vanderbilt.edu

[4] Abbreviations used in this paper: IKK2, IκB kinase 2; ARDS, acute respiratory distress syndrome; cIKK2, constitutively active human IKK2; DNTA, IκB-αDN-transactivated mice, transgenic mice expressing IκB-αDN under control of the CC10 promoter; dox, doxycycline; IκB-αDN, IκB-α dominant negative; IKTA, cIKK2-transactivated mice, transgenic mice expressing cIKK2 under control of the CC10 promoter; MTEC, mouse tracheal epithelial cell; RPA, RNase protection assay; rtTA, reverse tetracycline transactivator; tTS, tetracycline-controlled transcriptional silencer; WT, wild type.

epithelial cells is sufficient for generating acute lung injury, and inhibition of NF-κB activation in airway epithelium abrogates lung inflammation and injury induced by Gram-negative bacterial LPS. These findings suggest a paradigm in which airway epithelial cells control parenchymal lung inflammation and injury via production of NF-κB-dependent mediators.

Materials and Methods

Transgenic mouse models

IKTA-transgenic mice. The pBSIIFlag-IKK2 plasmid containing FLAG-cIKK2, a constitutively active form of human IKK2 containing S177E and S181E mutations, was a gift from Dr. F. Mercurio (Signal Pharmaceutical, San Diego, CA). This plasmid was digested with *Bss*HII to obtain a fragment containing the FLAG-IKK2. The ends of this fragment were filled in before ligation into the *Eco*RV site of a modified pBluescript II SK expression vector (pBSII KS/Asc). This vector contains a (tet-O)$_7$-CMV promoter that consists of seven copies of the tet operator DNA-binding sequence linked to a minimal CMV promoter together with bovine growth hormone polyadenylation sequences to ensure transcript termination. The final plasmid ((tet-O)$_7$-FLAG-cIKK2-BGH.poly(A)) was verified by sequencing. To prevent basal leakiness, we used a construct expressing a tetracycline-controlled transcriptional silencer (tTS) under control of the CC10 promoter (CC10-tTS-hGH-poly(A)) (10). The (tet-O)$_7$-FLAG-cIKK2 microinjection fragment was excised from the plasmid as a 3.3-kb *Xmn*I-*Asc*I fragment. We purified both CC10-tTS and (tet-O)$_7$-FLAG-cIKK2 constructs using a GELase Agarose Gel-Digesting preparation kit following the manufacturer's instruction (Epicentre), and these constructs were coinjected at the Vanderbilt transgenic/ES cell shared resource to generate transgenic lines of mice (FVB background) that have cointegrated both the CC10-tTS and (tet-O)$_7$-FLAG-cIKK2 transgenes. Genotyping of founder animals was performed by Southern Blot and later stages of genotyping were performed by PCR analysis. Primers used for PCR of the (tet-O)$_7$-FLAG-cIKK2 transgene are as follows: 5′ primer (located in the CMV minimal promoter) 5′-GAC GCC ATC CAC GCT GTT TTG-3′; and 3′ primer (located in the constitutively active form of IκB kinase 2 (cIKK2) coding region) 5′-CTT CTC ATG ATC TGG ATC TCC-3′. The product size is 452 bp. Primers used for identification of cc10-tTS transgene are as follows: upstream 5′-GAG TTG GCA GCA GTT TCT CC-3′; and downstream 5′-GAG CAC AGC CAC ATC TTC AA-3′. The product size is 472 bp. PCR protocols for both (tet-O)$_7$-FLAG-cIKK2 and CC10-tTS were as follows: 1 cycle 94°C for 2 min; 30 cycles at 94°C for 1 min, 56°C for 30 s, and 72°C for 1 min; and 1 cycle at 72°C for 10 min. Mice transgenic for CC10-tTS/(tet-O)$_7$-FLAG-cIKK2 were mated with cc10-rTTA homozygous mice (gift from Dr. J. A. Whitsett, University of Cincinnati, Cincinnati, OH) to obtain transgenic mice carrying all three transgenes, which were designated IKTA mice. IKTA mice from three separate founder lines were used for these studies.

IκB-αDN-transactivated (DNTA) transgenic mice. To tag the IκB-α dominant inhibitor (IκB-αDN) (8, 11, 12), a 1.35-kb *Bam*HI/*Dra*I fragment was excised from pCMX-pp40 and blunt-end ligated into *Bam*HI/*Eco*RV-digested pEF4/Myc-HisA (Invitrogen Life Technologies). The IκB-αDN-Myc-His-tagged fragment was then excised by *Bam*HI digest, fill-in of the overhanging ends and *Pme*I digestion. The resulting fragment was blunt-end ligated into the pBSII KS/Asc vector described above, which had been *Pst*I digested and filled in. Plasmid constructs were verified by sequencing. A 2.1-kb *Asc*I microinjection fragment was prepared and coinjected with the CC10-tTS microinjection fragment as described above at the Vanderbilt-transgenic/ES cell shared resource to generate transgenic lines of mice (FVB background) that have cointegrated both the CC10-tTS and (tet-O)$_7$-IκB-αDN-Myc-His transgenes. Genotyping of founder animals was performed by Southern blot analysis, and later stages of genotyping were performed by PCR analysis. Primers used for PCR of the (tet-O)$_7$-IκB-αDN-Myc-His transgene are as follows: sense primer, 5′-TGA GGA TGA GGA GAG CAG TGA ATC-3′; and antisense primer, 5′-CAC CCC CCA GAA TAG AAT GAC AC-3′. The product size is 422 bp. Primers used for identification of CC10-tTS transgene (as above). PCR protocols for (tet-O)$_7$-IκB-αDN-Myc-His was as follows: 1 cycle 95°C for 4 min; 30 cycles at 95°C for 30 s, 55°C for 30 s, and 72°C for 1 min; and 1 cycle at 72°C for 10 min. Mice transgenic for CC10-tTS/(tet-O)$_7$-IκB-αDN-Myc-His were mated with CC10-rTTA homozygous mice to obtain transgenic mice carrying all three transgenes, which were designated DNTA mice. DNTA mice from two separate founder lines were used for these studies.

Doxycycline (dox) treatment. All IKTA or DNTA mice (or appropriate controls) were maintained on normal water until transgene activation was desired. At that time, 2 g/L freshly prepared dox (Sigma-Aldrich) was added to the animals' drinking water. Sucrose (2%) was also added to decrease the bitter taste of dox water. The bottle with dox and 2% sucrose water was wrapped with foil to prevent light-induced dox degradation, and dox water was replaced twice per week.

LPS models

Male and female mice weighing between 20 and 25 grams were used for these studies. *Escherichia coli* LPS (serotype 055:B5) was obtained from Sigma-Aldrich. For studies involving aerosolized LPS, 8 ml of a 1 μg/μl LPS solution in PBS was delivered by ultrasonic nebulization in a closed chamber for 30 min using a previously published methodology (13). To deliver systemic LPS, an osmotic pump (2001D Alzet pump; ALZA) filled with LPS solution (1 μg/μl in PBS) was implanted surgically in the peritoneal cavity using sterile technique (9). The pump delivered 8 μg of LPS (8 μl)/h for 24 h. In some experiments, osmotic pumps (1003D) were used. These pumps were filled with LPS solution (8 μg/μl in PBS) to deliver 8 μg/h (1 μl/h) over 72 h. A priming dose of 3 μg of LPS/g body weight was injected i.p. following pump implantation.

Implantation of carotid artery catheter and blood gas analysis

The common carotid artery was separated from the vagus nerve and muscle, and then, two 6-0 silk threads were passed under the artery. The cephalic thread was tied to prevent bleeding, and then, the artery was clamped by small bulldog clamp. A small incision was made just below the ligature, and the catheter was inserted into the lumen. The clamp was taken off, and the catheter was pushed in 10 mm. The catheter was fixed with a second thread and the thread previously used to prevent bleeding. A blunt 16-gauge needle was carefully inserted through the incision and pushed s.c. until the end protruded through the incision in the neck. The incision in the skin was then sutured, and the catheter was connected to a stainless steel tube. The implanted catheter was flushed with saline containing 200 IU heparin/ml and 1 mg ampicillin/ml every day. For blood gas analysis, 100 μl of arterial blood was collected via the catheter and immediately placed in ice. Blood gas analysis was done using an ABL-5 blood gas machine (Radiometer America) at 37°C. Before each measurement, the blood gas machine was calibrated with a standard solution.

Lung histology and immunohistochemistry

Lungs were inflated and fixed with 1 ml of 10% formalin and then were removed en bloc after tracheal ligation. For immunohistochemical analysis, 5-μm paraffin sections were deparaffinized, dehydrated, washed with PBS, treated with 0.05% trypsin, and incubated with 1% BSA in PBS for 20 min before incubation with rabbit polyclonal anti-FLAG Ab (Rockland) or rabbit polyclonal anti-myc Ab (Santa Cruz Biotechnology). After incubation with primary Ab, a standard avidin-biotin complex protocol (Vectastain ABC kit; Vector Laboratories) using anti-rabbit secondary Abs was used. TUNEL assays were performed using a commercially available kit in accordance with the manufacturer's directions (In Situ Cell Death Detection kit; Roche Molecular Biochemicals). Semiquantitative scoring of TUNEL-positive cells was performed on histological specimens by a pathologist blinded to the genotype and treatment group. Ten sequential, nonoverlapping tissue fields of lung parenchyma were evaluated under ×400 magnification. Each tissue field was scored using a 0–4 point system (0, no positive cells; 1, ≤1% positive cells; 2, 1–5% positive cells; 3, 5–10% positive cells; and 4, 10–25% positive cells). A mean score for all fields was calculated for each animal.

EMSA

Tissue nuclear proteins were extracted from whole lung tissue by the method described previously (14). After preparation of nuclear protein extract, EMSA for NF-κB-binding activity was performed using oligonucleotides containing a consensus NF-κB-binding sequence (5′-AGT TGA GGG GAC TTT CCC AGG C-3′).

Western blot analysis

Protein extracts from tissue homogenates (100 μg) were separated on a polyacrylamide gel and transblotted for detection of FLAG-cIKK2 or IκB-αDN-Myc-His. For FLAG-cIKK2, proteins were separated on a 10% acrylamide gel, and anti-FLAG Abs (anti-FLAG conjugated with HRP M_2 mAb; Sigma-Aldrich) were used. HRP was detected by chemoluminescence using Lumi-Light^{PLUS} Western blotting substrate (Roche Diagnostics). For IκB-αDN-Myc-His, proteins were separated on a 12% polyacrylamide gel, and monoclonal anti-myc Abs (Sigma-Aldrich) were used for immunodetection. For detection of RelA in lung tissue nuclear protein fractions, nuclear proteins were prepared as previously described (14), 20 μg of protein was separated on a 10% acrylamide gel, and RelA was

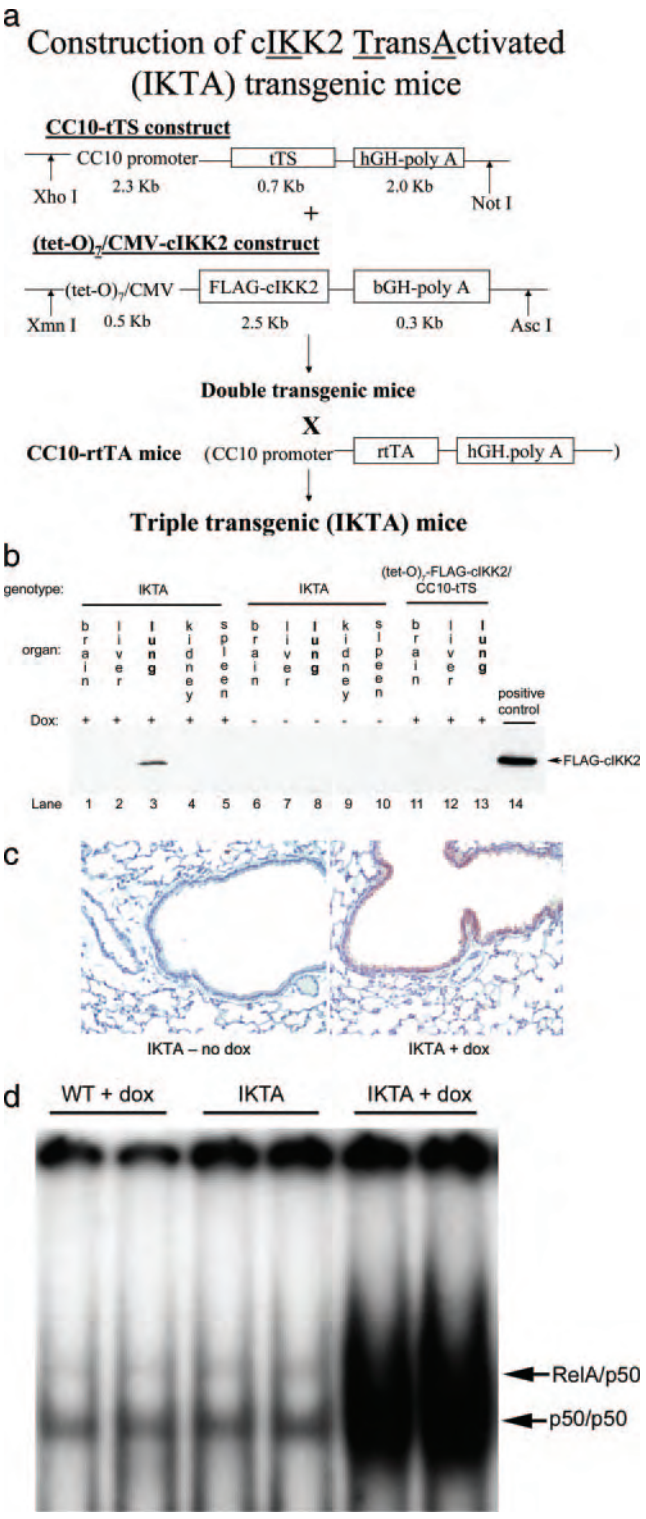

FIGURE 1. Dox-induced expression of FLAG-cIKK2 is localized to lung epithelial cells and sufficient to activate NF-κB. *a*, Schematic for construction of IKTA transgenic mice. *b*, Western blot analysis for FLAG-cIKK2 expression in tissue homogenates obtained from untreated IKTA mice, triple transgenic IKTA mice treated with dox for 3 days, or double transgenic (tet-O)$_7$-FLAG-cIKK2/CC10-tTS mice treated with dox. Transgene expression is detected only in the lungs of IKTA mice following dox treatment. *c*, Immunohistochemistry for FLAG in lung tissue from an untreated IKTA mouse (*left panel*) or an IKTA mouse treated with dox for 3 days (*right panel*). FLAG-cIKK2 staining (brown stain) is localized exclusively in airway epithelial cells in dox-treated IKTA mice. *d*, EMSA for NF-κB binding using lung nuclear protein extracts from WT control mice treated with dox (WT + dox), untreated IKTA mice (IKTA), and IKTA mice treated with dox for 3 days (IKTA + dox). Increased intensity of both NF-κB bands (RelA/p50 and p50/p50) is present in the IKTA + dox group.

immunodetected using rabbit polyclonal anti-RelA Abs (Santa Cruz Biotechnology). TATA-binding protein was detected as a loading control using specific Abs (Santa Cruz Biotechnology).

RNA isolation and RNase protection assay (RPA)

Lung tissue was homogenized in TRIzol reagent (Invitrogen Life Technologies), and RNA was isolated following the manufacturer's instructions. RPA using chemokine template mCK-5 was done with the RiboQuant multiprobe RPA system (BD Pharmingen) according to the manufacturer's direction.

Total and differential cell counts and protein measurement in lung lavage

Lung lavage was performed with 3 aliquots of 800 μl of sterile normal saline. Fluid was combined and centrifuged at 400 × *g* for 10 min to separate cells from supernatant. Supernatant was stored at −70°C for cytokine and chemokine measurements. The total and differential cell counts were done as described previously (12). Protein concentration was quantified using the Bradford assay (Bio-Rad).

Lung wet/dry ratio measurement

Lungs were removed and the wet weight recorded. Lungs were then placed in an incubator at 65°C for 48 h, and the dry weight was determined.

Cytokine and chemokine measurements

Measurement of cytokines and chemokines in lung lavage fluid and cell culture supernatant was done using the Bio-plex mouse cytokine 23-plex kit (Bio-Rad) following the manufacturer's direction and using Luminex technology. MIP-2 and KC levels were measured using a specific ELISA according to the manufacturer's instructions (R&D Systems).

Tracheal epithelial cell culture

Mouse tracheal epithelial cell (MTEC) culture was done by following the previously published protocol with minor modification (15). After removing muscle and vessels, tracheas were incubated in Ham's F-12 pen-strep containing 1.5 mg/ml pronase (Roche Molecular Biochemicals) for 18 h at 4°C to dislodge the epithelial cells. Cells were treated with 0.5 mg/ml crude pancreatic DNase I (Sigma-Aldrich) on ice for 5 min. After incubation in tissue culture plates (BD Biosciences) for 3–4 h in 5% CO_2 at 37°C to adhere fibroblasts, nonadherent cells were collected by centrifugation. Supported polycarbonate and polyester porous (0.4 μM pores) membranes (Transwell; Corning-Costar) were coated with type I rat tail collagen (BD Biosciences) in 0.02 N acetic acid for 18 h at 25°C. Membranes were seeded with cells and incubated with DMEM-Ham's F-12 medium containing 15 mM HEPES, 3.6 mM sodium bicarbonate, 4 mM L-glutamine, 100 U/ml penicillin, 100 μg/ml streptomycin, 0.25 μg/ml Fungizone, 10 μg/ml insulin, 5 μg/ml transferrin, 0.1 μg/ml cholera toxin, and 25 ng/ml epidermal growth factor (BD Biosciences) and 30 μg/ml bovine pituitary extract, 5% FBS, and freshly added 0.01 μM retinoic acid, filling upper and lower chambers in 5% CO_2 at 37°C. Media were changed every 2 days until the transmembrane resistance (R_t) was >1000 Ω · cm^2, as measured by an epithelial Ohm-voltmeter (World Precision Instruments). Media were then removed from the upper chamber to establish an air-liquid interface, and lower chambers only were provided fresh DMEM-Ham's F-12 medium supplemented with 2% NuSerum (BD Biosciences) and 0.01 μM retinoic acid.

Membrane cultures were prepared for scanning electron microscopy, as described previously (16). Briefly, samples were fixed with 2.5% glutaraldehyde, stained with 1.25% osmium tetroxide, critical point dried under liquid carbon dioxide, gold sputter coated, and visualized on a Hitachi S-3000N microscope (Hitachi).

For immunofluorescent detection of FLAG-cIKK2 expression, membranes were fixed with 4% paraformaldehyde (pH 7.4) for 10 min at 25°C and washed in PBS. A piece of membrane was cut and used for staining. Nonspecific Ab binding was blocked using 5% nonspecific serum and 3% BSA in PBS for 30 min at 25°C. Samples were incubated for 18 h at 4°C with anti-FLAG M2-FITC conjugate Ab (Sigma-Aldrich) in blocking solution. Membranes were mounted on slides with VectaShield (Vector Laboratories) containing 4′,6-diamidino-2-phenylindole to stain intracellular

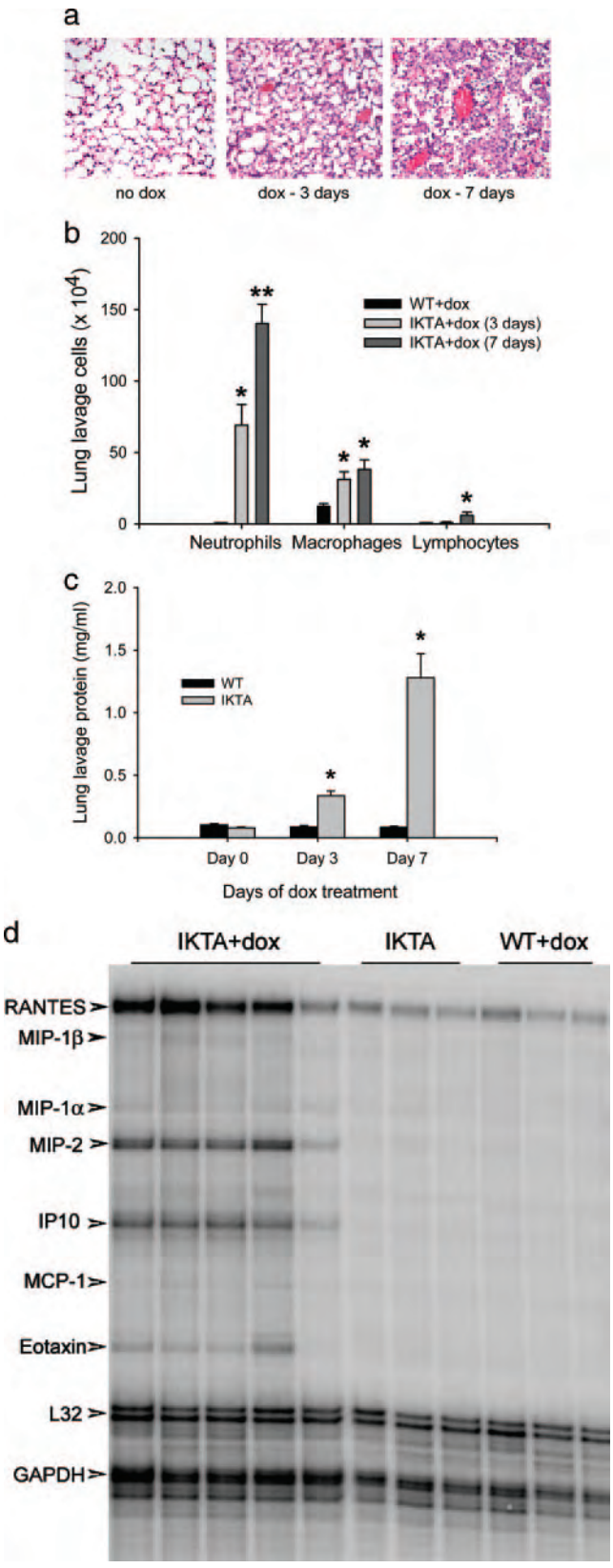

FIGURE 2. NF-κB activation in airway epithelium results in progressive lung inflammation and injury. *a*, H&E-stained lung sections from untreated IKTA mice and IKTA mice (line 3) treated with dox for 3 or 7 days. Although untreated IKTA mice have normal lung histology, a progressive inflammatory cell infiltrate is observed at 3 and 7 days after dox treatment, along with hemorrhage and edema at 7 days. *b*, Total neutrophils, macrophages, and lymphocytes in lung lavage from IKTA mice treated with dox for 3 or 7 days compared with WT mice treated with dox for 7 days ($n = 3$–4/group, $*$, $p < 0.05$ compared with WT, $**$, $p < 0.05$ compared with WT and IKTA mice treated with dox for 3 days). *c*, Lung lavage protein concentration in untreated WT and IKTA mice (day 0) and in both groups after 3 or 7 days of dox treatment ($n = 4$/group, $*$, $p < 0.01$ compared with WT). *d*, Multiprobe RNase protection assays for chemokines from lungs of IKTA or WT mice treated with dox for 7 days and IKTA mice without the addition of dox to drinking water. Each lane represents mRNA from a separate mouse.

Table I. *Lung lavage cytokine levels (picogram per milliliter)*[a]

	WT plus dox	IKTA (no dox)	IKTA plus dox
TNF-α	5.6 ± 3.4	4.6 ± 4.6	32.9 ± 11.0
IL-1α	1.3 ± 0.8	0	11.0 ± 2.3*
IL-1β	0	0	40.0 ± 1.6*
IL-2	12.6 ± 5.8	8.7 ± 1.6	25.8 ± 0.5
IL-5	1.0 ± 0.4	0.6 ± 0.6	12.8 ± 5.7*
IL-6	1.4 ± 0.9	1.2 ± 0.1	197.0 ± 54.0*
IL-9	17.9 ± 0	11.3 ± 10.2	31.6 ± 2.5
IL-10	1.5 ± 0.8	0	7.4 ± 2.6
IL-12p40	80.4 ± 9.5	28.2 ± 5.9	258.9 ± 83.3*
IL-17	1.1 ± 0.6	1.1 ± 0.6	13.7 ± 3.0*
Eotaxin	32.1 ± 26.3	44.8 ± 22.9	130.5 ± 18.6
RANTES	0	0	530.8 ± 106.0*
MIP-2	2.0 ± 0.6	0	35.4 ± 10.7*
MIP-1β	10.4 ± 0.8	11.1 ± 2.4	31.8 ± 9.2
KC	42.9 ± 3.7	65.3 ± 11.0	447.5 ± 125.4*
MCP-1	22.3 ± 10.1	12.1 ± 10.1	567.7 ± 144.2*
G-CSF	2.8 ± 0.4	9.6 ± 7.1	94.5 ± 9.1*
GM-CSF	6.8 ± 3.2	11.4 ± 2.9	37.9 ± 16.6

[a] Values measured by luminex or ELISA are presented as mean (±SEM). n = 3–5/group. $*$, $p < 0.05$ compared with all other groups by ANOVA. Levels of IL-3, IL-4, IL-12p70, IL-13, MIP-1α, and IFNγ were below the limits of detection.

DNA. The microscopic images were obtained by using a Zeiss LSM 510 confocal microscope (Zeiss).

Statistical analysis

To assess differences among groups, analyses were performed with GraphPad Instat (GraphPad) using an unpaired t test or one-way ANOVA. Mortality differences were evaluated using a Fisher's exact test. Results are presented as mean ± SEM. Two-tailed p values <0.05 were considered significant.

Results

Construction of transgenic mice with inducible activation of NF-κB in airway epithelium

To achieve inducible NF-κB activation using the tet-on system, we placed a FLAG-tagged cIKK2 (1) under control of the $(tet\text{-}O)_7$-CMV promoter (Fig. 1*a*). To prevent basal leakiness of transgene expression, a construct expressing tetracycline-controlled tTS under the control of the Clara cell-specific CC10 promoter (obtained from Dr. J. Elias, Yale University (New Haven, CT), with permission of A. Farmer, BD Clontech) was coinjected with $(tet\text{-}O)_7$-FLAG-cIKK2 to generate double transgenic mice. Unbound tTS interacts with tet-O sites and functions as a transcriptional repressor; however, binding of dox to tTS results in dissociation from DNA, allowing rtTA binding and promoter activation (10, 17, 18). Double transgenic mice were bred with transgenic mice expressing rtTA under the control of the rat CC10 promoter (obtained from Dr. J. A. Whitsett) to generate triple transgenic mice, which were designated IKTA (for cIKK2 transactivated).

In initial experiments, IKTA transgenic mice were treated with dox in drinking water (2 g/L) for 3 days. Western blots for the FLAG-tagged transgene product identified cIKK2 expression exclusively in the lungs of dox-treated IKTA mice (Fig. 1*b*). No leakiness of FLAG-cIKK2 expression was detectable in other

Table II. *Mediator concentration MTEC supernatant (picogram per milliliter)*[a]

	IKTA	IKTA plus dox
IL-1α	0	6 (4)
IL-1β	0	6 (1)
IL-6	11 (3)	554 (102)*
IL-12 (p70)	0	0
G-CSF	3247 (199)	9366 (460)*
GM-CSF	236 (61)	3816 (280)*
MIP-1α	0	0
MIP-2	121 (8)	833 (5)*
KC	9859 (507)	15908 (434)*
RANTES	242 (78)	14267 (632)*
TNF-α	0	0
IFN-γ	0	0

[a] Values measured by luminex or ELISA are presented as mean ($\pm$SEM). n = 3/group. *, $p < 0.05$ compared with IKTA cells (without dox treatment).

tissues following dox treatment or in the lungs in the absence of dox. By immunohistochemistry, FLAG-cIKK2 expression was localized to the airway epithelium (Fig. 1*c*). We investigated whether FLAG-cIKK2 expression in airway epithelium was sufficient to activate NF-κB by performing EMSAs using lung tissue nuclear protein extracts. Compared with controls, NF-κB activation was increased in lungs of dox-treated IKTA mice (Fig. 1*d*). Taken together, these data show that treatment of IKTA mice with dox induces expression of FLAG-cIKK2 exclusively in airway epithelial cells at levels sufficient to activate NF-κB.

Sustained NF-κB activation in airway epithelium results in neutrophilic lung inflammation and severe lung injury

Although untreated IKTA mice exhibited normal lung histology, IKTA mice showed progressive lung inflammation and injury after 3 and 7 days of dox treatment (Fig. 2*a*). After 3 days of dox treatment, lungs from IKTA mice showed evidence of edema and a cellular infiltrate consisting of neutrophils and macrophages. By 7 days of dox treatment, however, a massive infiltration of inflammatory cells into the lung parenchyma was present, along with septal thickening, edema, and alveolar hemorrhage. Other organs, including liver, spleen, and kidney, showed no evidence of inflammation or architectural abnormalities (data not shown).

By lung lavage, increased numbers of neutrophils and macrophages were identified in the airways of IKTA mice at 3 days after introduction of dox (Fig. 2*b*). After 7 days of dox treatment, increased numbers of neutrophils, macrophages, and lymphocytes were present in lung lavage from IKTA mice compared with dox-treated wild-type (WT) mice, and neutrophils were further elevated compared with IKTA mice treated with dox for 3 days. We measured protein concentration in lung lavage from IKTA mice and WT controls at baseline and after dox treatment as an indicator of vascular permeability (Fig. 2*c*). Compared with baseline, protein concentration in IKTA mice increased 3-fold by 3 days of dox treatment, and by day 7 of dox treatment, protein concentration had increased >10-fold above baseline. Lung lavage protein concentration was similar in untreated WT and IKTA mice and did not change in WT mice following dox treatment. Consistent with these results, wet/dry ratios were increased in dox-treated IKTA mice treated with dox for 3 days compared with controls (wet/dry ratio for WT mice 4.7 $\pm$ 0.1 for WT mice vs 5.7 $\pm$ 0.2 for IKTA, $p < 0.01$).

Activation of NF-κB in airway epithelium resulted in production of a variety of inflammatory mediators. Table I shows the profile of cytokines and chemokines up-regulated in lung lavage from IKTA mice treated with dox for 7 days compared with dox-treated WT mice and IKTA mice without dox treatment. Significantly increased levels of IL-1α, IL-1β, IL-5, IL-6, IL-12, IL-17, RANTES, MIP-2, KC, MCP-1, and G-CSF were observed in dox-treated IKTA mice. No differences in mediator production were identified between WT mice and IKTA mice in the absence of dox treatment. We used multiprobe RNase protection assays to confirm that mRNA expression of selected chemokines was increased in the lungs of dox-treated IKTA mice (Fig. 2*d*). Protein and mRNA measurements of mediators correlated well with the exception of MCP-1, which was increased in lung lavage fluid by Luminex assay, but increased mRNA expression was not identified in the lungs of dox-treated IKTA mice at this time point. Taken together, these studies show that sustained activation of NF-κB in IKTA mice (in the absence of a specific inflammatory stimulus) results in a pattern of progressive lung inflammation and injury associated with production of a number of NF-κB-regulated cytokines and chemokines.

To determine which inflammatory mediators are produced directly by airway epithelial cells following NF-κB activation, we harvested MTECs and grew them in air-liquid interface conditions to obtain highly differentiated airway epithelium (15). Cultures of MTECs from IKTA mice were treated with dox (0.5 μg/ml) for 48 h, and transgene induction was identified by immunostaining of

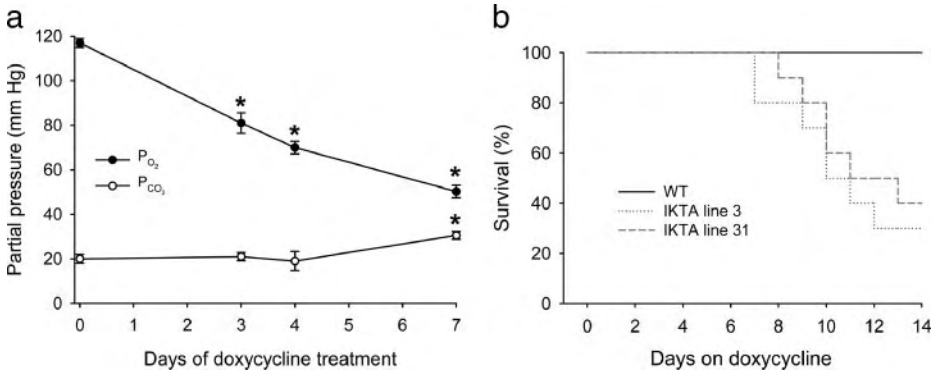

FIGURE 3. Treatment of IKTA mice with dox results in hypoxemia and increased mortality. *a*, Serial arterial blood gas measurements were obtained from indwelling carotid artery catheters. PO_2 and PCO_2 were assessed in IKTA mice at baseline and up to 7 days of dox treatment (n = 3–4/time point, *, $p < 0.01$ compared with baseline). *b*, Mortality rates in mice from IKTA lines 3 and 31 compared with WT controls through 14 days of dox treatment. Although all WT mice survived, 60% of mice in IKTA line 31 and 70% of mice in IKTA line 3 died between day 7 and 14 (n = 10 mice/group).

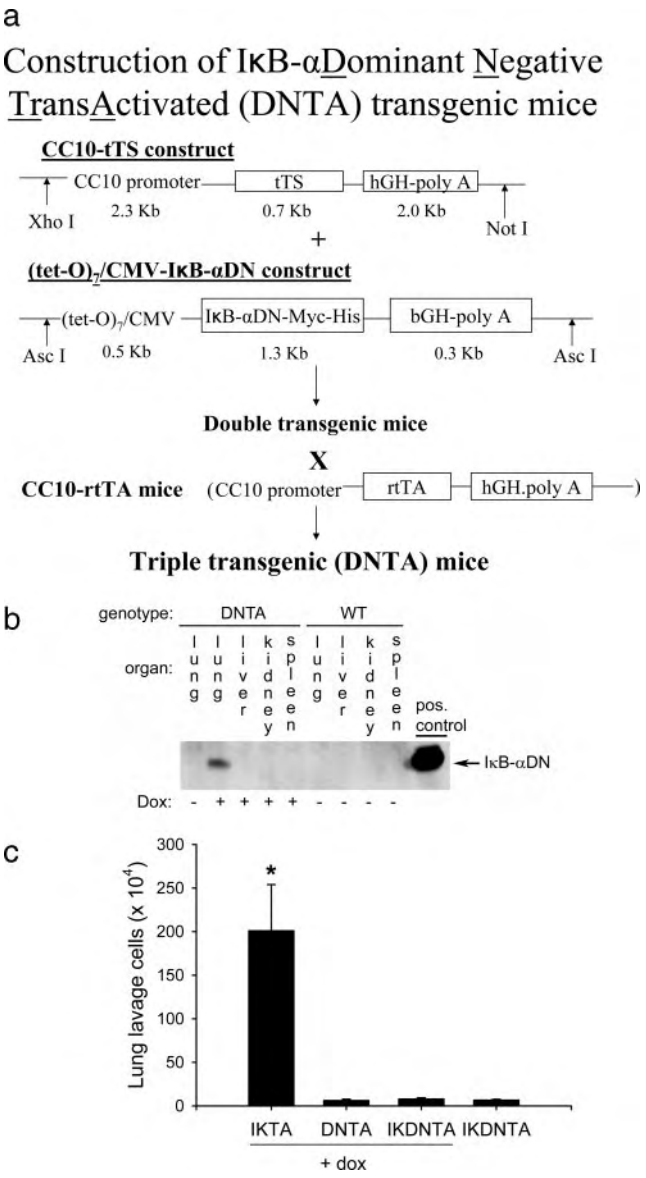

FIGURE 4. DNTA transgenic mice express a dominant inhibitor of the NF-κB pathway in airway epithelium. *a*, Schematic for construction of DNTA transgenic mice. *b*, Western blot analysis for Myc-His-tagged IκB-αDN expression in tissue homogenates obtained from WT and DNTA mice and DNTA mice treated with dox for 7 days. Transgene expression is detected only in the lungs of DNTA mice following dox treatment. *c*, DNTA mice were crossed with IKTA mice (line 26) to create IKDNTA mice that express both transgenes. Total cell counts in lung lavage are shown for IKTA mice (line 26), DNTA mice, and IKDNTA mice following 7 days of dox treatment and IKDNTA mice without dox treatment. The inflammatory cell influx was inhibited in dox-treated IKDNTA mice, indicating that expression of IκB-αDN blocks cIKK2-induced inflammation ($n = 4-8$/group, $*$, $p < 0.05$ compared with other groups).

FLAG-cIKK2 (data not shown). Increased concentrations of IL-6, G-CSF, GM-CSF, MIP-2, KC, and RANTES were identified in cell culture supernatants of dox-treated IKTA cells compared with IKTA cells in the absence of dox (Table II). These findings suggest that direct NF-κB activation in airway epithelial cells is sufficient to produce a number of mediators, including IL-6, G-CSF, MIP-2, KC, and RANTES, that are increased in the lungs of dox-treated IKTA mice. Other mediators that are increased in lung lavage fluid from dox-treated IKTA mice, such as IL-1α, IL-1β, and IL-12p40,

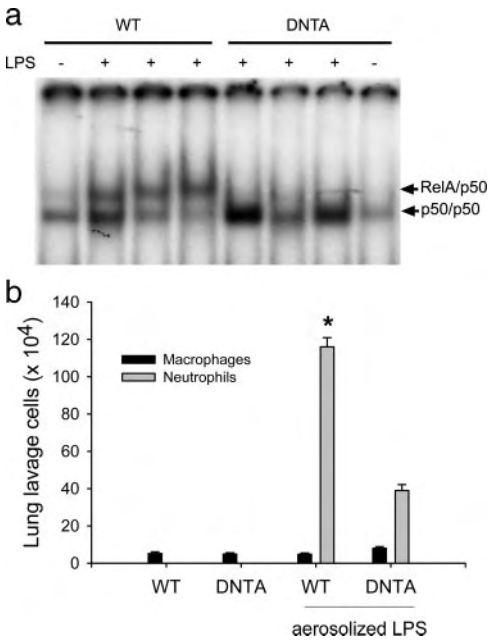

FIGURE 5. DNTA mice have reduced NF-κB activation and neutrophil influx into the airways after aerosolized LPS. WT or DNTA mice were given dox (2 g/L) in drinking water for 1 wk, treated with aerosolized LPS, and lungs were harvested 4 h later. *a*, EMSA for NF-κB binding using lung nuclear protein extracts indicates that induction of the RelA/p50 band is reduced in DNTA mice compared with WT in LPS-treated mice. *b*, Lung lavage cell counts show that LPS-induced neutrophil recruitment is inhibited in DNTA mice ($n = 3$/group, $*$, $p < 0.05$ compared with other groups).

may be up-regulated indirectly through recruitment or activation of inflammatory cells in the lungs.

We sought to determine the physiological effects of lung inflammation/injury resulting from epithelial NF-κB activation in IKTA mice by measuring arterial PO_2. Serial arterial blood gas analysis was done with indwelling carotid artery catheters in unanesthetized IKTA mice treated with dox (Fig. 3*a*). Baseline PO_2 (123.9 ± 4.67 mm Hg) and PCO_2 (20.1 ± 0.93 mm Hg) in IKTA mice were similar to WT controls (data not shown). With continued dox treatment, arterial PO_2 in IKTA mice decreased to 50.3 ± 2.81 mmHg by day 7 and PCO_2 increased to 30.5 ± 4.33 mm Hg. Arterial oxygen saturation decreased from 99 ± 0.1% at baseline to 81 ± 2.7% after 7 days of dox treatment in IKTA mice ($p < 0.001$). WT controls with indwelling carotid artery catheters treated with dox for 1 wk did not show any changes from baseline in arterial PO_2, PCO_2, or arterial oxygen saturation (data not shown).

Continued dox treatment resulted in substantial mortality in IKTA mice between 1 and 2 wk (Fig. 3*b*). In two separate lines of IKTA mice, mortality rates of 60 and 70% were found by 2 wk of dox treatment, whereas no mortality was observed in WT control mice treated with dox for 2 wk. Taken together, these studies demonstrate that persistent induction of NF-κB in airway epithelial cells is sufficient to cause lung inflammation and injury. Lung injury in this model results in progressive hypoxemia with a high mortality rate.

Construction and characterization of transgenic mice that express a dominant inhibitor of NF-κB in airway epithelium

We placed a Myc-His tagged dominant inhibitor of the NF-κB pathway (IκB-αDN) under control of the (tet-O)$_7$-CMV promoter (Fig. 4*a*). IκB-αDN is an avian IκB-α with adenine substitutions at serines 36 and 40 that inhibit phosphorylation and degradation of the protein, therefore blocking NF-κB nuclear translocation (8, 11,

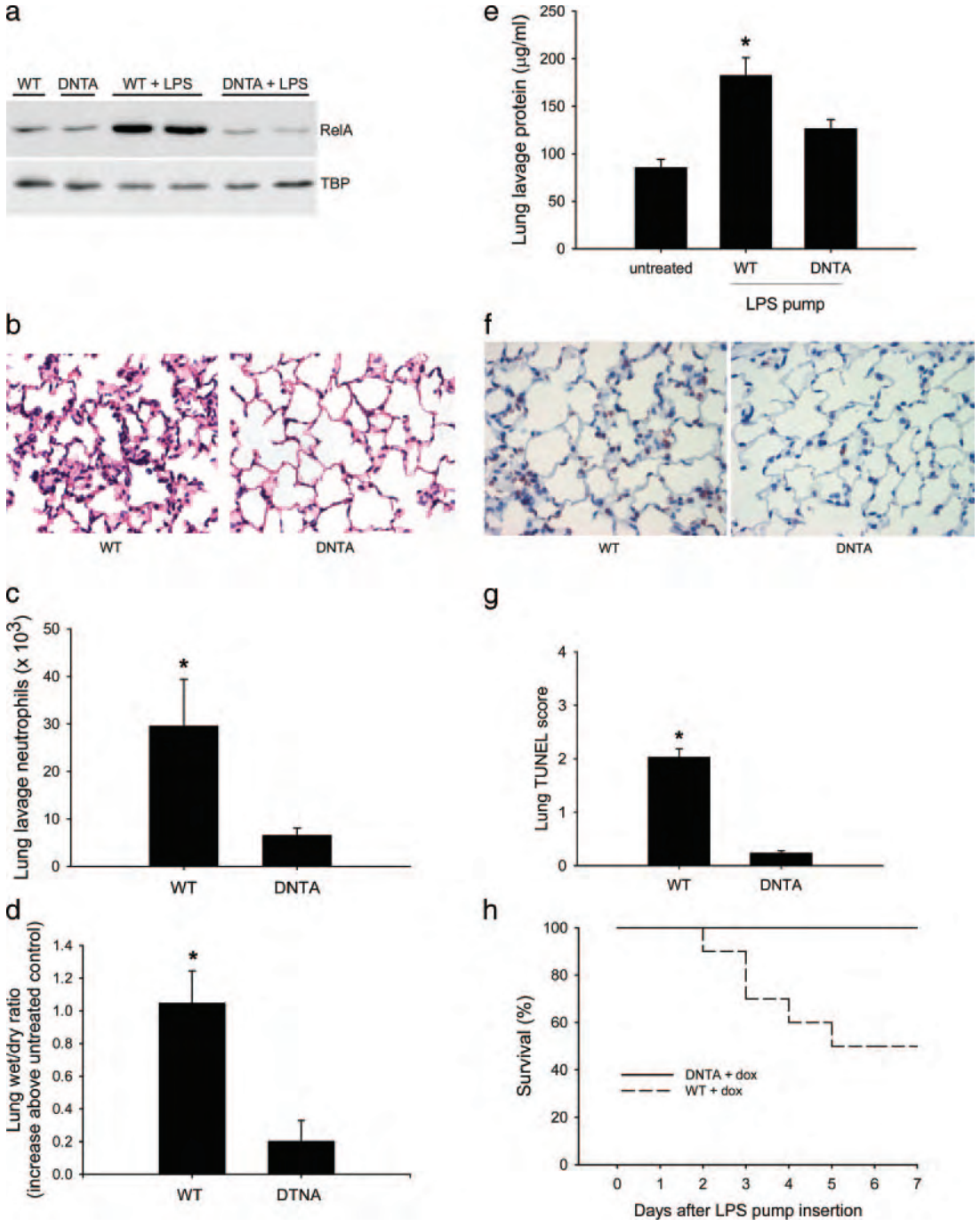

FIGURE 6. DNTA mice are protected from *E. coli* LPS-induced lung inflammation and injury. WT or DNTA mice were treated with dox (2 g/L) in drinking water for 1 wk, followed by i.p. implantation of osmotic pumps delivering LPS. *a*, Western blot analysis from lung nuclear protein extracts showing impaired nuclear translocation of RelA in DNTA mice at 4 h after LPS pump implantation (DNTA + LPS) compared with WT mice (WT + LPS). Samples from DNTA mice and WT mice without LPS pumps are shown as controls. TATA binding protein (TBP) was identified as a loading control. *b*, H&E-stained lung sections from WT and DNTA mice harvested 48 h after i.p. placement of pumps that deliver LPS continuously for 24 h. Lung inflammation and edema were markedly reduced in dox-treated DNTA mice. *c*, Lung lavage neutrophils obtained at 48 h after LPS pump placement ($n = 10$/group; $*$, $p < 0.05$). *d*, Lung wet/dry ratios for WT and DNTA mice treated with LPS pumps presented as increase above untreated controls ($n = 10$/group, $*$, $p < 0.01$). *e*, Lung lavage protein concentration in untreated WT mice and WT and DNTA mice at 48 h after treatment with LPS pump ($n = 6$/group, $*$, $p < 0.05$ compared with untreated mice and LPS pump-treated DNTA mice). *f* and *g*, Representative photomicrographs of TUNEL staining (brown nuclear stain) and scoring of TUNEL$^+$ cells in lung parenchyma from WT and DNTA mice at 48 h after treatment with LPS pumps ($n = 8$/group, $*$, $p < 0.05$). *h*, Mortality rates in dox-treated WT and DNTA mice following i.p. implantation of osmotic pumps that deliver LPS at 8 μg/h over 72 h ($n = 10$/group, $*$, $p < 0.05$).

12). Double transgenic mice containing (tet-O)$_7$-IκB-αDN-Myc-His and CC-10-tTS constructs were produced and cross-mated with CC10-rtTA mice to create triple transgenic mice with inducible expression of IκB-αDN-Myc-His in airway epithelium, which were designated DNTA (for IκB-αDN transactivated). As with IKTA mice, dox treatment resulted in transgene expression exclusively in the lungs (Fig. 4*b*). No leakiness of transgene expression was identified in the absence of dox. Immunohistochemistry for

Table III. *Mediators in lung lavage at baseline and 48 h after implantation of LPS pump (picogram per milliliter)*[a]

	WT	DNTA	WT (plus dox) plus LPS	DNTA (plus dox) plus LPS
TNF-α	0	0	22.7 ± 17.7	1.2 ± 0.5
IL-1α	1.7 ± 0.6	1.8 ± 0.1	81.1 ± 9.3	61.1 ± 6.2
IL-1β	0	0	10.2 ± 6.1	3.7 ± 1.6
IL-2	0	0	24.2 ± 2.4	12.4 ± 4.1**
IL-3	0	0	2.7 ± 0.6	1.0 ± 0.5
IL-5	0	0	3.6 ± 1.1	1.6 ± 0.3
IL-6	0	0	16.2 ± 2.2	9.3 ± 2.2
IL-9	0	0	170.0 ± 31.0	93.0 ± 20.0
IL-10	0	0	7.7 ± 2.8	0
IL-12p40	32.4 ± 5.4	17.8 ± 5.5	65.2 ± 19.1	49.0 ± 10.4
IL-12p70	0	0	8.6 ± 3.8	4.1 ± 2.0
Eotaxin	0	0	76.0 ± 39.3	10.7 ± 10.4
RANTES	2.3 ± 0.8	1.1 ± 0.4	31.8 ± 2.8	19.1 ± 3.0**
MIP-2	0	0	21.9 ± 3.2	4.1 ± 1.5**
MIP-1β	0	0	33.8 ± 8.9	8.9 ± 2.6**
KC	60 ± 3.3	25.0 ± 2.2*	696 ± 77	290 ± 36**
MCP-1	24.3 ± 8.1	16.2 ± 9.3	668 ± 134	288 ± 59**
G-CSF	1.5 ± 0.5	1.9 ± 0	16,597 ± 5,651	2,729 ± 509**
GM-CSF	0	0	23.3 ± 5.3	9.7 ± 2.5**
IFNγ	0	0	8.7 ± 5.4	6.0 ± 3.0

[a] Values measured by luminex or ELISA are presented as mean (±SEM). $n = 4$ mice/group at baseline and 6/group after LPS pump. *, $p < 0.05$ compared with WT group at baseline; **, $p < 0.05$ compared with WT group treated with LPS pumps. Levels of IL-4, IL-13, IL-17, and MIP-1α were below the limits of detection.

the Myc tag on IκB-αDN localized transgene expression to the airway epithelium in dox-treated mice (data not shown). Lungs of dox-treated DNTA mice were histologically normal.

To show that IκB-αDN expression was sufficient to block NF-κB activation in DNTA mice, we crossed IKTA and DNTA mice to obtain mice that inducibly expressed both transgenes (cIKK2 and IκB-αDN-Myc-His). Fig. 4*c* shows that dox treatment of these mice (IKDNTA) results in suppression of lung inflammation induced by cIKK2. These experiments indicate that expression of IκB-αDN in epithelium inhibits NF-κB activation and confirm that cIKK2-induced lung inflammation is transduced through activation of the NF-κB pathway.

Prevention of lung inflammation and injury by blocking NF-κB activation in airway epithelium

After demonstrating that expression of IκB-αDN in epithelial cells blocks NF-κB activation, we undertook studies to identify the effects of inhibiting epithelial NF-κB following treatment with *E. coli* LPS. Initially, WT and DNTA mice were treated with dox for 1 wk to induce transgene expression and then were administered aerosolized *E. coli* LPS (8 ml of a 0.1 μg/ml solution) as reported previously (13). At 4 h after LPS treatment, lungs were lavaged and harvested for determination of neutrophilic alveolitis and NF-κB activation by EMSA. As shown in Fig. 5*a*, dox treatment of DNTA mice reduced nuclear translocation of RelA/p50 heterodimers (the transactivating component of NF-κB) in lung tissue following treatment with aerosolized LPS. Neutrophil influx into the airways was also diminished in DNTA mice (Fig. 5*b*). These findings show that expression of IκB-αDN blocks NF-κB activation and neutrophil recruitment induced by aerosolized LPS.

In addition to direct airway exposure to LPS, we investigated whether blocking NF-κB activation in airway epithelium could reduce lung inflammation and injury resulting from systemic delivery of *E. coli* LPS. We used a model of abdominal sepsis in which LPS is delivered into the peritoneum (8 μg/h) over 24 h via a surgically implanted osmotic pump (9). Using transgenic NF-κB reporter mice, we have recently shown that this model results in persistent lung NF-κB activation that prominently involves airway epithelium (9). For these studies, we treated WT or DNTA mice with dox for 1 wk, followed by implantation of the LPS pump. At 4 h after osmotic pump implantation, NF-κB activation was reduced in DNTA mice as indicated by Western blots for RelA in lung nuclear protein extracts (Fig. 6*a*). At 48 h after implantation, WT mice exhibited histological evidence of lung injury with edema and inflammatory cell influx, which was markedly reduced in DNTA mice (Fig. 6*b*). Consistent with these findings, lung lavage neutrophils were reduced in DNTA mice (Fig. 6*c*). In addition, total lung lavage cells were lower in dox-treated DNTA mice than controls at 48 h after placement of LPS pumps ($16.5 \pm 1.6 \times 10^4$ cells in DNTA mice compared with $35.0 \pm 4.6 \times 10^4$ cells in WT mice, $n = 10$/group, $p < 0.01$). No differences in peripheral white blood cell counts were identified between dox-treated WT and DNTA mice at baseline, 4 h, or 48 h after placement of LPS pumps (data not shown). WT and DNTA mice treated with LPS pumps in the absence of dox treatment had BAL cell counts and peripheral white blood cell counts similar to dox-treated WT mice (data not shown).

We performed multiplex cytokine analysis to evaluate the effects of epithelial NF-κB inhibition on the mediator profile in lung lavage fluid obtained at the time of harvest (Table III). Untreated WT and DNTA mice were included as controls. At 48 h after implantation of LPS pumps, levels of MIP-2 and KC were lower in dox-treated DNTA mice than in dox-treated WT mice, which is consistent with the reduced neutrophilic lung inflammation observed in these mice. Other mediators that were reduced in DNTA mice included RANTES, MIP-1β, MCP-1, G-CSF, and GM-CSF.

At 48 h after implantation of LPS pumps, evidence of disruption of the alveolar capillary barrier was present in dox-treated WT mice with increased lung wet/dry ratios and increased protein concentration in lung lavage compared with control mice in the absence of LPS treatment. Dox-treated DNTA mice, however, were almost completely protected from edema and protein leak after LPS treatment (Fig. 6, *d* and *e*). WT and DNTA mice treated with LPS pumps in the absence of dox treatment had lung wet/dry ratios that were similar to dox-treated WT mice (data not shown). Because disruption of the alveolar-capillary barrier has been linked to

apoptosis of structural cells (both epithelium and endothelium) in lung parenchyma (19–21), we investigated whether LPS-induced alveolar cell death was reduced in DNTA mice compared with WT. As shown in Fig. 6, *f* and *g*, a striking difference in $TUNEL^+$ cells was identified in the lung parenchyma of WT and DNTA mice at 48 h after LPS pump implantation. Frequent $TUNEL^+$ structural and inflammatory cells were identified in lungs of dox-treated WT mice, whereas very few $TUNEL^+$ cells were identified in dox-treated DNTA mice (Fig. 6*f*). Semiquantitative analysis of lung sections from mice treated with dox, followed by LPS pumps, showed a significant reduction in the number of $TUNEL^+$ cells in lungs of DNTA mice compared with WT mice (Fig. 6*g*). TUNEL scores were similar in LPS-treated WT mice with or without dox treatment, and both DNTA and WT mice had very few $TUNEL^+$ cells in lung parenchyma in the absence of LPS treatment (data not shown). Because transgene expression was limited to bronchial epithelium in DNTA mice (as detected by immunohistochemistry), it appears that protection from apoptosis in alveolar cells of DTNA mice is an indirect effect of reduced inflammatory signaling through the NF-κB pathway in airway epithelium.

To determine whether reduced lung injury in DNTA mice could lead to improved survival, we performed peritoneal implantation of osmotic pumps that deliver LPS (8 μg/h) for 72 h into dox-treated WT and DNTA mice. As shown in Fig. 6*h*, delivery of LPS over 72 h resulted in 50% mortality in WT mice at day 7; however, all dox-treated DNTA mice survived.

Discussion

These studies describe the generation, characterization, and use of a novel modular transgenic system that enables regulation of NF-κB activity in specific cell populations. By using this approach to specifically target the NF-κB pathway in airway epithelium, we have defined a pivotal role for epithelial cells in controlling lung inflammation and injury. In DNTA mice, expression of a dominant NF-κB inhibitor in CC10 expressing cells reduces neutrophilic lung inflammation resulting from airway or systemic delivery of LPS and diminishes lung injury and mortality following endotoxemia. In complementary studies using IKTA-transgenic mice, we show that IKK2 expression causes persistent activation of NF-κB in airway epithelial cells, resulting in cytokine production, inflammatory cell recruitment, lung injury, hypoxemia, and high mortality. In IKTA mice, dox treatment induces progressive lung injury with inflammation and edema by 3 days, followed by impaired gas exchange and death after as few as 7 days. Since the onset of detectable transgene expression occurs by 24–48 h after adding dox to drinking water (data not shown), induction of lung injury in dox-treated IKTA mice occurs in a time frame similar to that observed in the systemic LPS model. Taken together, our studies suggest a paradigm in which inflammatory signaling in airway epithelium plays a critical role in orchestrating the lung's response to LPS (and possibly other injurious stimuli) delivered either locally (via the airways) or systemically (via the bloodstream). In this model, the NF-κB pathway in airway epithelium is a focal point for control of lung injury through regulated production of mediators that participate in recruitment/activation of inflammatory cells, induction of alveolar cell death, and disruption of the alveolar capillary barrier.

Although a large number of studies have investigated regulation of inflammatory responses to environmental stress through the NF-κB pathway, the majority of these studies have focused on NF-κB signaling in immune cells. In the lungs, NF-κB is activated in macrophages early after LPS treatment (22), and macrophages are required for maximal activation of NF-κB in the whole lung and the resulting neutrophil influx (23, 24). This information suggests that alveolar macrophages are required for initiation of LPS-induced inflammatory responses in the lungs, likely through activation of NF-κB signaling. However, our data and another recent study (25) indicate that NF-κB signaling in nonimmune cells is critical for determining the lung's response to injurious stimuli. Kisseleva et al. (25) expressed a dominant inhibitor of the NF-κB pathway in endothelial cells using the Tie2 promoter and found that NF-κB blockade resulted in increased vascular permeability in the lungs, increased endothelial apoptosis, and increased mortality in response to systemic LPS. Based on these findings, LPS-induced NF-κB activation in endothelium appears to be primarily protective through maintenance of vascular integrity. In contrast, NF-κB signaling in airway epithelial cells leads to increased vascular permeability in the lungs, and inhibiting LPS-induced NF-κB activation in these cells reduces lung inflammation, edema, and alveolar cell death. Therefore, targeting of NF-κB pathway in specific cell types or compartments (like the airways) may be necessary to effectively reduce lung inflammation and injury.

Previous studies have suggested that lung epithelial cells impact neutrophil recruitment through NF-κB pathway signaling. We found that intratracheal administration of adenoviral vectors expressing NF-κB-activating transgenes in mice results in neutrophilic inflammation (11). Mice deficient in RelA, the primary transactivating component of NF-κB, and TNFR1 exhibit a marked reduction of neutrophilic inflammation in response to airway delivery of LPS (26). In contrast, bone marrow chimeras in which the RelA/TNFR1 deficiency is limited to immune cells (including lung macrophages) have normal LPS-induced neutrophil recruitment, implicating non-bone marrow-derived cells in generation of neutrophilic inflammation in this model. In addition, transgenic mice constitutively expressing a NF-κB inhibitor in lung epithelial cells have reduced neutrophil influx into the airways in response to intranasal instillation of *E. coli* LPS (27, 28). In the gastrointestinal tract, selective deletion of IKK2 in intestinal epithelial cells impairs NF-κB activation and results in decreased lung and systemic inflammation in a gut ischemia-reperfusion model through reduction of TNF-α expression (29). However, local tissue injury in the intestinal mucosa is exacerbated in this model related to increased apoptosis. In combination with the present study, these findings point to the NF-κB pathway in epithelial cells as an important target for therapies designed to modulate inflammation-induced tissue injury.

In humans, evidence supports the role of NF-κB-dependent mediators in inducing lung injury, although the cellular source of these mediators is not well defined. A variety of NF-κB linked cytokines and chemokines has been reported to be increased in lung lavage fluid obtained from patients with ARDS, including TNF-α, IL-1β, IL-6, and IL-8 (6, 30, 31). Increased concentrations of IL-8, a NF-κB-regulated CXC chemokine in humans, are found in lungs of at-risk patients who progress to ARDS, and high levels of IL-8 and neutrophils in lung lavage have been correlated with increased mortality in ARDS patients (32–34). Our mouse model indicates that prolonged activation of NF-κB in epithelial cells is sufficient to produce an inflammatory profile similar to human ARDS, as well as the pathophysiological and histological abnormalities. These findings solidify the NF-κB pathway as an important therapeutic target for interventions targeted to limit lung injury in ARDS. It is intriguing to note that the relatively small percentage of lung cells that constitute the airway epithelium appear to have the potential to play a powerful protective role against lung injury. Airway epithelial cells are relatively accessible to aerosolized agents, and specific inhibition of NF-κB activity by this route could leave intact host defense mechanisms mediated by inflammatory cells in the lung.

In summary, our findings support three major conclusions. First, we have generated a modular transgenic system that can be used to efficiently modulate NF-κB activity in specific cell types. These mice have the potential to be used in a broad range of future research endeavors. Second, our findings implicate the NF-κB pathway in airway epithelial cells is critical for generation of lung inflammation and injury in response to local and systemic stimuli. Indeed, persistent NF-κB activation in epithelium may provide a common pathway for driving the dysregulated inflammatory response that culminates in ARDS. Third, while interventions that reduce inflammation by blocking NF-κB activation in epithelium must be rigorously examined to define their effects on host defense, the airway epithelium may prove to be an important and feasible target for reducing or preventing lung injury in patients at risk for ARDS.

Acknowledgments

We thank Dr. Jeffrey A. Whitsett of the University of Cincinnati College of Medicine for the donation of CC-10 rtTA-expressing transgenic mice used in these studies. We also thank the Vanderbilt University Mouse Metabolic Phenotyping Core, the Vanderbilt Transgenic/ES Shared Resource, and the Mouse Pathology Core for their valuable assistance.

Disclosures

The authors have no financial conflict of interest.

References

1. Mercurio, F., H. Zhu, B. W. Murray, A. Shevchenko, B. L. Bennett, J. Li, D. B. Young, M. Barbosa, M. Mann, A. Manning, and A. Rao. 1997. IKK-1 and IKK-2: cytokine-activated IκB kinases essential for NF-κB activation. *Science* 278: 860–866.
2. Blackwell, T. S., and J. W. Christman. 1997. The role of nuclear factor-κB in cytokine gene regulation. *Am. J. Respir. Cell Mol. Biol.* 17: 3–9.
3. Ghosh, S., M. J. May, and E. B. Kopp. 1998. NF-κB and Rel proteins: evolutionarily conserved mediators of immune responses. *Annu. Rev. Immunol.* 16: 225–260.
4. Ware, L. B., and M. A. Matthay. 2000. The acute respiratory distress syndrome. *N. Engl. J. Med.* 342: 1334–1349.
5. Kollef, M. H., and D. P. Schuster. 1995. The acute respiratory distress syndrome. *N. Engl. J. Med.* 332: 27–37.
6. Bhatia, M., and S. Moochhala. 2004. Role of inflammatory mediators in the pathophysiology of acute respiratory distress syndrome. *J. Pathol.* 202: 145–156.
7. Muir, A., G. Soong, S. Sokol, B. Reddy, M. I. Gomez, A. Van Heeckeren, and A. Prince. 2004. Toll-like receptors in normal and cystic fibrosis airway epithelial cells. *Am. J. Respir. Cell Mol. Biol.* 30: 777–783.
8. Sadikot, R. T., H. Zeng, M. Joo, M. B. Everhart, T. P. Sherrill, B. Li, D. S. Cheng, F. E. Yull, J. W. Christman, and T. S. Blackwell. 2006. Targeted immunomodulation of the NF-κB pathway in airway epithelium impacts host defense against *Pseudomonas aeruginosa*. *J. Immunol.* 176: 4923–4930.
9. Everhart, M. B., W. Han, T. P. Sherrill, M. Arutiunov, V. V. Polosukhin, J. R. Burke, R. T. Sadikot, J. W. Christman, F. E. Yull, and T. S. Blackwell. 2006. Duration and intensity of NF-κB activity determine the severity of endotoxin-induced acute lung injury. *J. Immunol.* 176: 4995–5005.
10. Zhu, Z., B. Ma, R. J. Homer, T. Zheng, and J. A. Elias. 2001. Use of the tetracycline-controlled transcriptional silencer (tTS) to eliminate transgene leak in inducible overexpression transgenic mice. *J. Biol. Chem.* 276: 25222–25229.
11. Sadikot, R. T., W. Han, M. B. Everhart, O. Zoia, R. S. Peebles, E. D. Jansen, F. E. Yull, J. W. Christman, and T. S. Blackwell. 2003. Selective I κB kinase expression in airway epithelium generates neutrophilic lung inflammation. *J. Immunol.* 170: 1091–1098.
12. Blackwell, T. S., F. E. Yull, C. L. Chen, A. Venkatakrishnan, T. R. Blackwell, D. J. Hicks, L. H. Lancaster, J. W. Christman, and L. D. Kerr. 2000. Multiorgan nuclear factor κB activation in a transgenic mouse model of systemic inflammation. *Am. J. Respir. Crit. Care Med.* 162: 1095–1101.
13. Yull, F. E., W. Han, E. D. Jansen, M. B. Everhart, R. T. Sadikot, J. W. Christman, and T. S. Blackwell. 2003. Bioluminescent detection of endotoxin effects on HIV-1 LTR-driven transcription in vivo. *J. Histochem. Cytochem.* 51: 741–749.
14. Blackwell, T. S., T. R. Blackwell, and J. W. Christman. 1997. Impaired activation of nuclear factor-κB in endotoxin-tolerant rats is associated with down-regulation of chemokine gene expression and inhibition of neutrophilic lung inflammation. *J. Immunol.* 158: 5934–5940.
15. You, Y., E. J. Richer, T. Huang, and S. L. Brody. 2002. Growth and differentiation of mouse tracheal epithelial cells: selection of a proliferative population. *Am. J. Physiol.* 283: L1315–L1321.
16. Look, D. C., M. J. Walter, M. R. Williamson, L. Pang, Y. You, J. N. Sreshta, J. E. Johnson, D. S. Zander, and S. L. Brody. 2001. Effects of paramyxoviral infection on airway epithelial cell Foxj1 expression, ciliogenesis, and mucociliary function. *Am. J. Pathol.* 159: 2055–2069.
17. Deuschle, U., W. K. Meyer, and H. J. Thiesen. 1995. Tetracycline-reversible silencing of eukaryotic promoters. *Mol. Cell. Biol.* 15: 1907–1914.
18. Forster, K., V. Helbl, T. Lederer, S. Urlinger, N. Wittenburg, and W. Hillen. 1999. Tetracycline-inducible expression systems with reduced basal activity in mammalian cells. *Nucleic Acids Res.* 27: 708–710.
19. Martin, T. R., N. Hagimoto, M. Nakamura, and G. Matute-Bello. 2005. Apoptosis and epithelial injury in the lungs. *Proc. Am. Thorac. Soc.* 2: 214–220.
20. Kawasaki, M., K. Kuwano, N. Hagimoto, T. Matsuba, R. Kunitake, T. Tanaka, T. Maeyama, and N. Hara. 2000. Protection from lethal apoptosis in lipopolysaccharide-induced acute lung injury in mice by a caspase inhibitor. *Am. J. Pathol.* 157: 597–603.
21. Fujita, M., K. Kuwano, R. Kunitake, N. Hagimoto, H. Miyazaki, Y. Kaneko, M. Kawasaki, T. Maeyama, and N. Hara. 1998. Endothelial cell apoptosis in lipopolysaccharide-induced lung injury in mice. *Int. Arch. Allergy Immunol.* 117: 202–208.
22. Blackwell, T. S., L. H. Lancaster, T. R. Blackwell, A. Venkatakrishnan, and J. W. Christman. 1999. Differential NF-κB activation after intratracheal endotoxin. *Am. J. Physiol.* 277: L823–L830.
23. Koay, M. A., X. Gao, M. K. Washington, K. S. Parman, R. T. Sadikot, T. S. Blackwell, and J. W. Christman. 2002. Macrophages are necessary for maximal nuclear factor-κB activation in response to endotoxin. *Am. J. Respir. Cell Mol Biol.* 26: 572–578.
24. Lentsch, A. B., B. J. Czermak, N. M. Bless, N. Van Rooijen, and P. A. Ward. 1999. Essential role of alveolar macrophages in intrapulmonary activation of NF-κB. *Am. J. Respir. Cell Mol. Biol.* 20: 692–698.
25. Kisseleva, T., L. Song, M. Vorontchikhina, N. Feirt, J. Kitajewski, and C. Schindler. 2006. NF-κB regulation of endothelial cell function during LPS-induced toxemia and cancer. *J. Clin. Invest.* 116: 2955–2963.
26. Alcamo, E., J. P. Mizgerd, B. H. Horwitz, R. Bronson, A. A. Beg, M. Scott, C. M. Doerschuk, R. O. Hynes, and D. Baltimore. 2001. Targeted mutation of TNF receptor I rescues the RelA-deficient mouse and reveals a critical role for NF-κB in leukocyte recruitment. *J. Immunol.* 167: 1592–1600.
27. Poynter, M. E., C. G. Irvin, and Y. M. Janssen-Heininger. 2003. A prominent role for airway epithelial NF-κB activation in lipopolysaccharide-induced airway inflammation. *J. Immunol.* 170: 6257–6265.
28. Skerrett, S. J., H. D. Liggitt, A. M. Hajjar, R. K. Ernst, S. I. Miller, and C. B. Wilson. 2004. Respiratory epithelial cells regulate lung inflammation in response to inhaled endotoxin. *Am. J. Physiol.* 287: L143–L152.
29. Chen, L. W., L. Egan, Z. W. Li, F. R. Greten, M. F. Kagnoff, and M. Karin. 2003. The two faces of IKK and NF-κB inhibition: prevention of systemic inflammation but increased local injury following intestinal ischemia-reperfusion. *Nat. Med.* 9: 575–581.
30. Goodman, R. B., R. M. Strieter, D. P. Martin, K. P. Steinberg, J. A. Milberg, R. J. Maunder, S. L. Kunkel, A. Walz, L. D. Hudson, and T. R. Martin. 1996. Inflammatory cytokines in patients with persistence of the acute respiratory distress syndrome. *Am. J. Respir. Crit. Care Med.* 154: 602–611.
31. Schutte, H., J. Lohmeyer, S. Rosseau, S. Ziegler, C. Siebert, H. Kielisch, H. Pralle, F. Grimminger, H. Morr, and W. Seeger. 1996. Bronchoalveolar and systemic cytokine profiles in patients with ARDS, severe pneumonia and cardiogenic pulmonary oedema. *Eur. Respir. J.* 9: 1858–1867.
32. Miller, E. J., A. B. Cohen, S. Nagao, D. Griffith, R. J. Maunder, T. R. Martin, J. P. Weiner-Kronish, M. Sticherling, E. Christophers, and M. A. Matthay. 1992. Elevated levels of NAP-1/interleukin-8 are present in the airspaces of patients with the adult respiratory distress syndrome and are associated with increased mortality. *Am. Rev. Respir. Dis.* 146: 427–432.
33. Donnelly, S. C., R. M. Strieter, S. L. Kunkel, A. Walz, C. R. Robertson, D. C. Carter, I. S. Grant, A. J. Pollok, and C. Haslett. 1993. Interleukin-8 and development of adult respiratory distress syndrome in at-risk patient groups. *Lancet* 341: 643–647.
34. Baughman, R. P., K. L. Gunther, M. C. Rashkin, D. A. Keeton, and E. N. Pattishall. 1996. Changes in the inflammatory response of the lung during acute respiratory distress syndrome: prognostic indicators. *Am. J. Respir. Crit. Care Med.* 154: 76–81.